DEVELOPING SMART GROUTED SAND COLUMNS FOR REAL TIME MONITORING OF THE STABILITY, SEEPAGE AND RAPID DRAWDOWN IN EARTH DAMS

A Thesis

Presented to

the Faculty of the Department of Civil & Environmental Engineering

University of Houston

In Partial Fulfillment

of the Requirements for the Degree

Master of Science

in Civil Engineering

by

Halil Ibrahim Kula

December 2016

DEVELOPING SMART GROUTED SAND COLUMNS FOR REAL TIME MONITORING OF THE STABILITY, SEEPAGE AND RAPID DRAWDOWN IN EARTH DAMS

Halil Ibrahim Kula

Approved:

Chair of the Committee
Cumaraswamy Vipulanandan, Professor,
Civil and Environmental Engineering

Committee Members:

Yi-Lung Mo, Professor,
Civil and Environmental Engineering

Gino J. Lim, Professor,
Industrial Engineering

Suresh K. Khator, Associate Dean,
Cullen College of Engineering

Roberto Ballarini, Professor and Chair,
Civil and Environmental Engineering

ACKNOWLEDGEMENTS

I would like to express my greatest gratitude to my supervisor, Dr. C. Vipulanandan, who directed all stages of my research program with his professional guidance and academic advice. This work could not be successfully completed without him. I would also like to thank Dr. Yi-Lung Mo and Dr. Gino J. Lim for their participation of the defense committee.

Appreciation is also expressed to GEM Group members for their help. Thank you for your encouragement and your beneficial discussions that provided me the strength to move forward.

I would like to send my deepest gratitude to my family, Ramazan and Necla Kula. Thank you for your love and moral support. Lastly, I appreciate the General Directorate of State Hydraulic Works (DSI), Turkey, for financial support.

DEVELOPING SMART GROUTED SAND COLUMNS FOR REAL TIME MONITORING OF THE STABILITY, SEEPAGE AND RAPID DRAWDOWN IN EARTH DAMS

An Abstract

of a

Presented to

the Faculty of the Department of Civil & Environmental Engineering

University of Houston

In Partial Fulfillment

of the Requirements for the Degree

Master of Science

in Civil Engineering

by

Halil Ibrahim Kula

December 2016

ABSTRACT

The reservoir drawdown can negatively affect the upstream slope stability of earth dams due to removal of the balancing hydraulic forces acting on the dams during undrained condition in the soil. Therefore, monitoring upstream slope during rapid drawdown is an important task in terms of stability. Having lower wetting zone inside the earth dam using low permeability materials can provide a good design for earth dams and prevent possible failures which is related to seepage problems.

In this study, acrylamide grouted sand was used to monitor upstream slope during rapid drawdown and control the seepage inside the earth dam. To better characterize the behavior, over 140 grouted sand specimens were prepared with different particle size of sands. Particle size, gradation, and compaction affected the compressive strength of grouted sands. The compressive strength of the grouted sands varied from 240 kPa to 775 kPa after 7 days of moist curing. Also, the curing time after 3 days did not affect the mechanical properties of the grouted sands. Nonlinear Vipulanandan p-q constitutive model was used to predict the mechanical behavior of acrylamide grouted sands. The permeability of grouted sand was 10^{-12} m/sec, and it was not affected by grain size distribution and particle size.

Electrical resistivity was identified as the sensing and monitoring property for the acrylamide grouted sands. The acrylamide grouted sand with and without conductive filler were piezoresistive. Electrical resistivity change was identified as the sensing and monitoring property for the acrylamide grouted sands. 0.1% conductive filler (CF) was added to make the grouted sands very sensitive under water submerged and moist conditions. Adding CF increased piezoresistivity from 10% to 21%. Nonlinear Vipulanandan p-q constitutive model was used to predict the piezoresistive behavior of the grouted sands. Assigning acrylamide grouted sand to upstream face decreased phreatic line in the earth dam and seepage quantity and increased the stability of earth dam twice compare to clay core.

In this study, the potential use of grouted sand in installation was numerically investigated using an earth dam 2-D model. Seepage and stability analysis were performed during rapid drawdown condition and change in shear stress were quantified. Shear stress change was used to check the piezoresistivity of acrylamide grouted sand columns used in the model embankment. Based on the changes in the electrical resistivity for real-time monitoring, location for the piezoresistive grouted sand columns were identified.

TABLE OF CONTENTS

LIST OF FIGURES

TABLE OF CONTENTS

CHAPTER 1 INTRODUCTION

General

Earth dam is an artificial barrier that is constructed to retain water. Dams are mainly constructed for retention of water in a confined and used for water supply, flood control, irrigation, energy production, recreation and fishing (ICOLD). They are mainly classified into four parts according to their structure types (Ersayin, 2006). These are gravity, buttress, embankment and arch dams. Dams which are built using earth materials, are commonly referred to earthfill dams. There are 11.192 earthfill dams around the world according to Foster (2000).

When it comes to designing embankment dams, stability and seepage control are required for dam safety. When there is no enough or suitable clay material in the dam area, embankment dams are constructed with two permeable shells and with impermeable core in the middle (Athani, 2015). The reasons for failures in embankment dams are generally referred to following reasons such as; seepage failure, piping through dam body, hydraulic failure and structural damage due to earthquake effect (Osuji, S.O., 2015).

Designing, planning, and constructing of a dam requires great attention and care. Even dams are constructed according to criteria or standards, continuous monitoring during the lifetime of the dams must be a factor to be considered. Physical parameters which are related to deformations, stress, and water level must be monitored. The measurements made along with visual inspection and supervision, can provide early warning of any type of failure.

One of the main problem with earth dam is seepage. Seepage line which is referred to as phreatic line is used to understand the degree of seepage. The phreatic line level in the dams affects the stability of the dam (Osuji, S.O., 2015). Since saturation zone which is below this line will have positive hydrostatic pressure, the flow will reduce the shear strength of the soil due to pore-water pressure (Osuji, S.O., 2015).

Polymeric grouts have been used for stopping water leaks in cracks and fractures and also stabilizing earth materials for decades (Drochytka, 2016). The advantages of the chemical grout are having low viscosity to minimize the pumping pressure, controllable gelling time, ability to make the medium impermeable with enough strength (Ozgurel, 2005).

Objectives

The overall objective of this study is to investigate the behavior of acrylamide grouted sands used for earth dams. The specific objectives of this study are:

a) To study the effect of particle size and distribution on the mechanical, permeability and sensing properties (piezoresistivity, moisture content) of acrylamide grouted sands.

b) To investigate the effectiveness of acrylamide grouted sand in earth dam for real-time monitoring and seepage control.

Organization

This thesis is organized into 6 chapters. In chapter 2, literature review related to the monitoring systems and seepage problem are summarized. Methods of monitoring earth dams and seepage control methods are documented. In Chapter 3, materials used for preparing the acrylamide grouted sand samples and experimental procedures are broadly discussed. It also provides the necessary theory and information about the testing methods used. Chapter 4 addresses the mechanical, permeability and piezoresistivity behavior of acrylamide grouted sands when various particle size and distribution sands are used. Chapter 5 focuses on the model verification of monitoring dam and controlling seepage line in the earth dam using acrylamide grout. Chapter 6 summarizes the conclusions that have been reached from this study, and recommendations for future research.

.

CHAPTER 2 BACKGROUND AND LITERATURE REVIEW

Introduction

Dams are a hydraulic structure that is build to store water in the river. Generally it is constructed of earth and rock materials and they have to be designed to make the most effective use with reasonable cost (Ersayin, 2006). Moreover, dams are constructed for several uses such as water supply, irrigation, flood control and produce hydroelectric power (Novak, 2001). They are mainly classified into four parts according to their structure types. In order to select a type of dam, there are some factors are considered such as site conditions, topography, geology and foundation conditions, material available, environmental and economic situation (USACE, 2004). Around 52% of the world`s dams are located in China, 16% in the United States, and 6% in Japan (Bequette, 1997). Main components of a typical dam is shown in Figure 2-1.

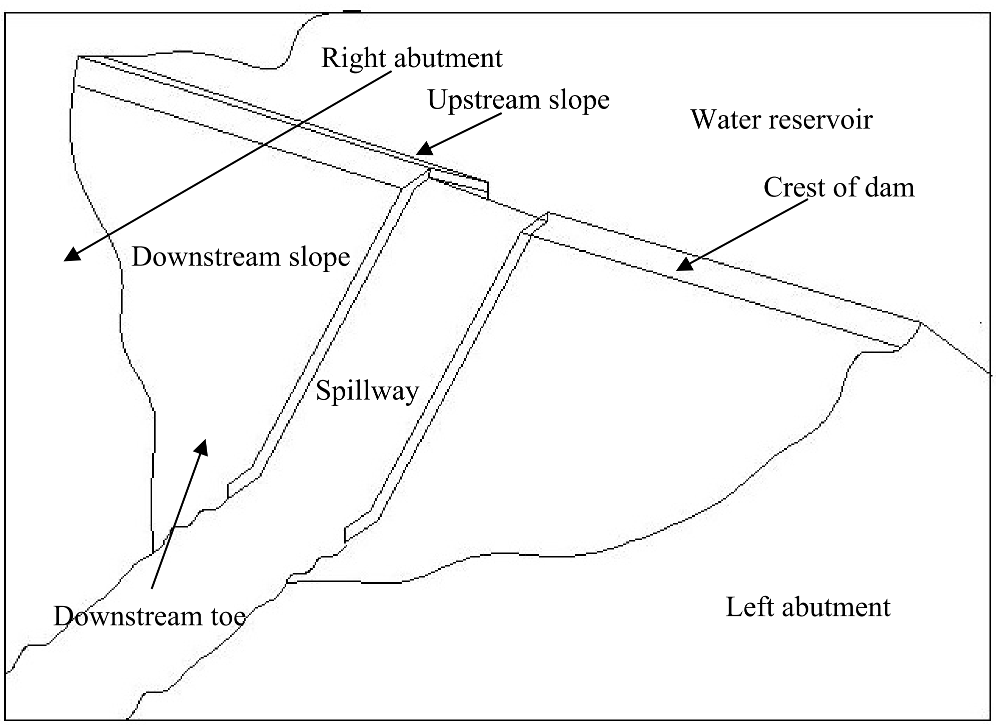

Figure 2-1:Typical Main Components of Dam

All dams are designed and constructed to meet specific criteria and standards. First, locally available materials are important factor to construct a dam. Second, the dam must stand stable under all conditions, during construction and in operation. The most important another thing is to control seepage in the dam body and its` foundation. Thus, stability of the dam against slope failure and seepage control in the dam are an essential components for the design.

Main Functions of Dams

According to International Commision on Large Dams (ICOLD), main functions of dams can be summarized as follows: water supply, flood control, water storage, producing electricity, irrigation, and recreation. Figure 2-2 shows the percentage applications for earth dams.

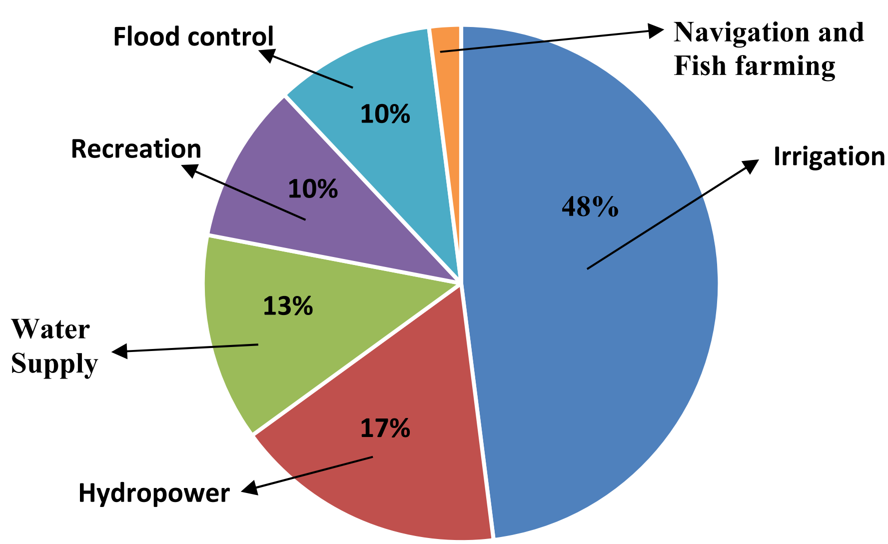

Figure 2-2:Applications for Earth Dams

History of the Dams

The history of building earth dams is much older than concrete type of dams (Narita, 2000). According to reliable records, the first dam was built in Jordan 5,000 years ago to supply drinking water in the city of Jaw (Ersayin, 2006). A large dam was built by an Arabian king called Lokman about 1700 B.C. and it collapsed due to flooding (Ersayin, 2006). The oldest existing dams in Europe which were constructed before 1586 are the Almanza and Alicante dams in Spain (Ersayin, 2006). Earth dams which has the height of more than 15m are called "high dams" according to International Commision on Large Dams (ICOLD). According to existing dams records, about 14000 high dams have been constructed up to the 2000, and 70% of dams are earth type of dam (Narita, 2000). Therefore, a last report has noted that among around 1000 of high dams constructed in recent two years, 80 percent of them are earth dams (Narita, 2000). In the United States, there is an organization called The World Register of Dams (WRD) that is registering dams in the world. According to its` 2011 records there are 37.500 dams are high dams. For each dam, they have more than 30 statistical information. Moreover, the WRD is an important source of information for scientifical work, statistical evaluations, design, and construction for earth dams (Mai, 2004).

Types of Dams

Basically, dams are classified on the structure types, usage purposes and materials of construction (Ersayin, 2006). According to their structures, they can be classified four categories such as gravity dams, arch dams, buttress dams and embankment dams. Classification of the dams are summarized in Table 2-2.

Table 2-1:Classification of Dams

According to structure	On the basis of the materials of construction	According to usage purposes
1-) Gravity Dams 2-) Arch Dams 3-) Buttress Dams 4-) Embankment Dams a-) Earth Dams b-) Rockfill Dams	1-)Masonry Dams a-) Stone and Brick Dams b-) Concrete Dams c-) Reinforced Concrete Dams 2-) Filling Dams a-) Earthfill Dams b-) Rockfill Dams 3-) Masonry and Filling Dams 4-) Framed Dams a-) Steel Dams b-) Timber Dams	1-) Dams for drinking water 2-) Dams for Industrial water 3-) Dams for Irrigation 4-) Dams for flood control 5-)Dams for hydroelectric power 6-) Cofferdams

Embankment Dams

Embankment dams can be divided into two types as earthfill and rockfill dams. Foster (2000) have reported that there are 11.192 embankment dams were constructed up to 1986. Moreover, up to 1986 62% of dams are designed with zoned earthfill dam. Table 2-1 has showed the number of embankment dams that were constructed up to 1986. Figure 2-3 has showed different type of embankment dams.

Table 2-2:Number of Embankment Dams Around the World During Different Time Periods Foster (2000)

Embankment types	Before 1900	1900-1930	1930-1950	1950-1970	1970-1986	All years
Homogeneous earthfill	101	172	444	1641	1320	3469
Zoned earthfill	240	573	641	2439	2728	6939
concrete face earthfill and rockfill	22	73	82	355	352	783
Total	363	818	1167	4335	4400	11192

Earthfill dams

An earth dam is constructed partly or completely using pervious material which consist of clay, silt or mixture of clay, silt and gravel. In order to construct an economical dam, materials are taken from available excavation in a site. Homogeneous earthfill dams are constructed using similar materials. This type of dam has to have enough permeability to control seepage inside the dam and the slope must be relatively flat for stability (DSI, 2012). Moreover, in order to prevent leakage in the core, filter zone is constructed to transfer water to upstream (DSI,2012).

Homogeneous earthfill dam is generally constructed for dam which is less than 30m in height. However, if dam has to be constructed with higher than 30 m, filter design must be performed to drop phreatic line in upstream and downstream zones (DSI, 2012).

Rockfill Dams

This type of dam is constructed with a mass of dumped rock. Impermeable layer can be provided by clay core, inclined core or facing. Filter layers are performed on the clay core upstream and downstream face. Clay core is supported by shell zones. There are three type of rockfill dams such as rockfill dam with a centrally located core, rockfill dam with an inclined core and rockfill dam with a facing (DSI, 2012).

The forces acting on dams

Main forces are acting on the dams can be summarized as follows.

Water Pressure

Water pressure is on the upstream face of the structure. There is an important factor that must be included in the also when silt builds up the lower part of the upstream side the dam, it moves as a liquid that is denser than water (Ersayin, 2006).

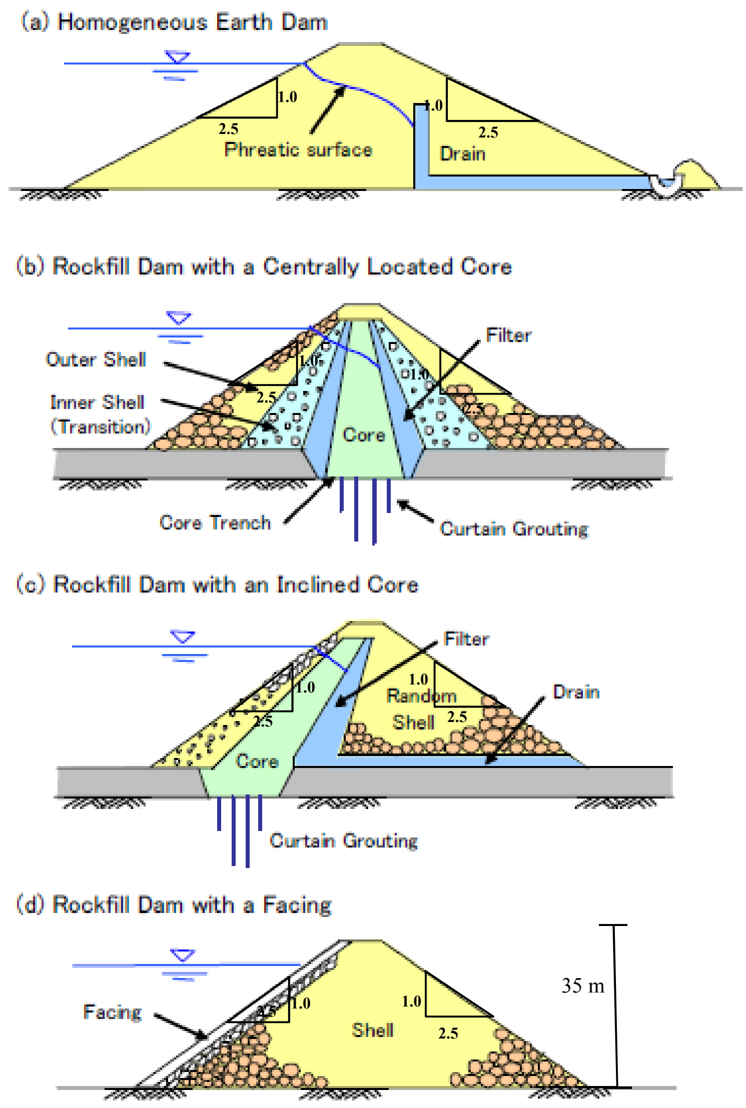

Figure 2-3:Earthfill and Rockfill Dams (a) Homogeneous Earth Dam, (b) Rockfill Dam with a Centrally Located Core, (c) Rockfill Dam with a Inclined Core Clay Earth, and (d) Rockfill Dam with a Facing

Dam Weight

The weight of the dam itself is another force that acts on the dam structures. Moreover, exterrior forces that are coming from bridges or gates are add weight to the dam.

Earthquakes

The horizontal and vertical seismic forces must be taken into consideration when designing a dam. When earthquake occurs toward upstream to downstream, soil and water pressure increases towards downstream. Additionally, weight of the dam caused ineartial forces to downstream in the horizontal direction. In order to calculate earthquake forces, intensity of earthquake must be known. Its value is typically expressed in terms of the acceleration of gravity.

Ice

Ice pressure, temperature and ice thickness is calculated based on the growth rate (Berkun, 2005). Temperature changes in the dam and ice thickness can be estimated from from meteorological data. Ice pressure depending on the climate and the location of the dam reservoir can be varied 0 – 75 t/m (Berkun, 2005).

Failures and Damages in Earth Dams

Internal erosion and piping resulting from seepage are the biggest problems affecting the stability of earthfill dams (Fattah, 2014). According to Foster (2000) investigation, piping causes 43% of failures in the earth dams. Also, the same study showed that 66% of piping problems was due to seepage in the dam body.

Due to improper designs, faulty constructions, lack of maintance, and natural cases , earth dams may fail. Piping, concentrated leak erosion, contact erosion and suffusion has the reasons of internal erosion (ICOLD 2012). Several different types of failures and damages of earthfill dams have been summarized as shown in Table 2-3 and Figure 2-2. There are three factors that cause to failures of earthen dams (Garg, 2006). These are as follows:

- Hydraulic failure
- Seepage failure
- Structural failure

Hydraulic failure has caused about 40% of earth dam failures (Osuji, S.O., 2015). The hydraulic failure is due to over topping, erosion of upstream face and downstream toe that was seen in the New Orleans during hurricane Katrina. Uncontrolled seepage through dam body of its foundation may lead to piping or sloughing (Osuji, O.S., 2015). More than 1/3 of earth dams have failed due to piping (Garg, 2006). Structural failures are generally caused by shear failure which is causing sliding and this failure has caused about 25% of the dam failures (Garg, 2006).

Seepage in Earth Dams and the Importance of Seepage in Dam`s Body

The most important thing that affects dam stability negatively is the seepage problem. This seepage can make dam`s body weak and cause a sudden failure due to piping or sloughing. An earthfill dam`s body stops water flow inside the dam from upstream to downstream. However, even using impermeable zone inside the dam body, there will be some water seeps into dam`s body and the flow goes out from downstream of body slope until it meets an impermeable zone (Ersayin, 2006). So if the water level at the upstream is lowered rapidly, saturated soil in the upstream may become unstable. This issue has to be considered when designing an earth dam. Generally, earthfill dams are designed pervious and some seepage flow through the dam body must be considered.

Phreatic Line in Earth Dams

Phreatic line is defined as the line below which there is a saturated soil which has positive hydrostatic pressures above this line has negative pressures and the hydrostatic pressure on this line is equal to atmospheric pressure. So there is a pore water pressure under this line. According to seepage analysis, there are several reasons that affect the value of water pore pressure. These factors include, permeability of soil, and load on soil. Hence below the phreatic line the effective weight of soil is decreased, and thus reduces shear strength of the soil due to positive pore water pressure then soil will tend to move (Osuji, O.S., 2015). This process called piping. Piping usually occurs near the downstream toe of a dam when seepage excessive (Linsley and Franzini, 1964). Hence there is need to improve the stability of the embankment below the phreatic line.

Methods of Seepage Control

All earth and rockfill dams will be subject to seepage through the foundations, abutments, and embankments (Osuji, O.S., 2015). To prevent excessive uplift pressures, unstability of the upstream and downstream slope, piping through the dam body or foundation and erosion of material is necessary for seepage control. There are at least three methods that can be used to control seepage in dam body such as vertical and horizontal drains, flat slopes without drains and impermeable zonation (Osuji, O.S., 2015). Upstream impervious barriers, cutoffs, downstream seepage berms, relief wells, and trench drains are also control seepage methods for foundation of the dam (EM, 2004).

Monitoring for Earth Dams

Determining the performance of earthfill dams is related to the weight of the dam body, stress and deformation resulting from hydrostatic pressure and seepage quantity (Taymaz, and Yildiz, 1993). The purpose behind monitoring and maintance is for the earth dams and also ensure the general stability of dam during construction or end of the construction, and ensure there is no internal erosion or piping resulting from seepage during the service life. Measurements made for monitoring earthfill dams can be as follows (EM-1110-2-1004, EM-1110-2-1908).

- Horizontal-vertical deformations
- Determining ground water level and pore water pressure
- Shear and total stress and strain measurements
- Seepage quantities measurements
- Seismic movements
- Visual measurements
- Phreatic surface line

Instrumentation in Earthfill Dams

Dams are large structures and they have to be monitored with instruments in there lifespan (DSI, 2012). Needed data and instrumentation must be carefully planned to acquire the needed data. Information that instrumentation gives can be summarized as follows;

- Description of site condition before construction.
- Ensuring proper materials used.
- Ensuring proper construction and design followed.
- Verifying design and analysis assumptions.
- Observation of geologic and structural abnormal performance that is known
- Transferring data for future structures.

Instruments used in earth dams can be summarized as follows:

Piezometers

It is used for monitoring seepage in the foundation of dam, ground water level, effectiveness of cutoff wall, and measuring pore water pressure in the foundation. Suggested locations are shown in Figure 2-5. (DSI, 2012). Moreover, accuracy of piezometers is ± 0.5% according to DSI.

Inclinometers

It is used for monitoring lateral earth movements, detecting movement of downstream of earth fill dam, particularly impounding, monitoring stability of upstream during and after impounding as shown in Figure 2-5. (Knight, 2016). Moreover depth, direction, magnitude and rate of movement can be taken from inclinometers. Inclinometers help to locate shear zone and identify whether shear is planner of circular. It can be located center of the crest or center of upstream slope. Accuracy of inclinometers is ±2 mm per 25 m.

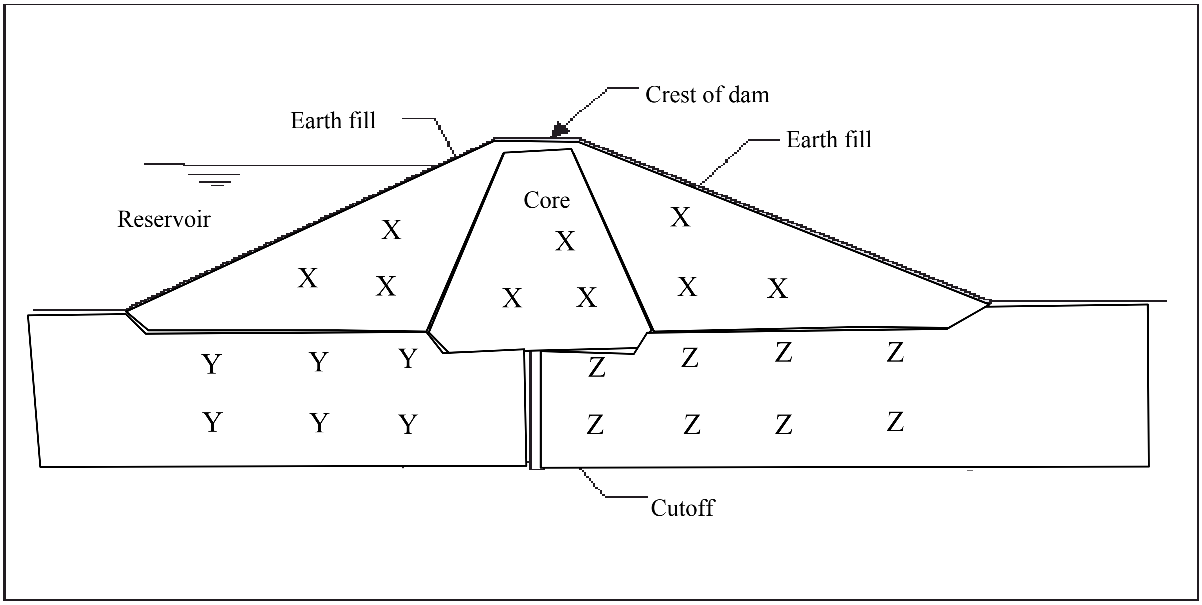

Figure 2-4:Suggested Locations for Piezometers in Earthfill Dams

As shown in Figure 2.4, the place named Y shows to check placement of fill, monitor porewater pressure to find shear strength. Z shows to control placement of fill, monitor pwp to find shear strength and measure uplift pressure and monitor seepage. X shows to control placement of fill and monitor seepage.

Settlement cell

As shown in Figure 2-6, it is located upstream, downstream slope and core of the dam (DSI, 2012). It is applicable for three direction to measure deformations. It is used for monitoring consolidation during construction and long term settlement in the foundation of the fill. Accuracy of settlement cells is ± 0.5%.

Extensometers

It is located in the toe of the upstream as shown in Figure 2-7. (Knight, 2016). It is used for monitoring vertical deformations in the dam body. Accuracy of extensometers is ± 0.25%.

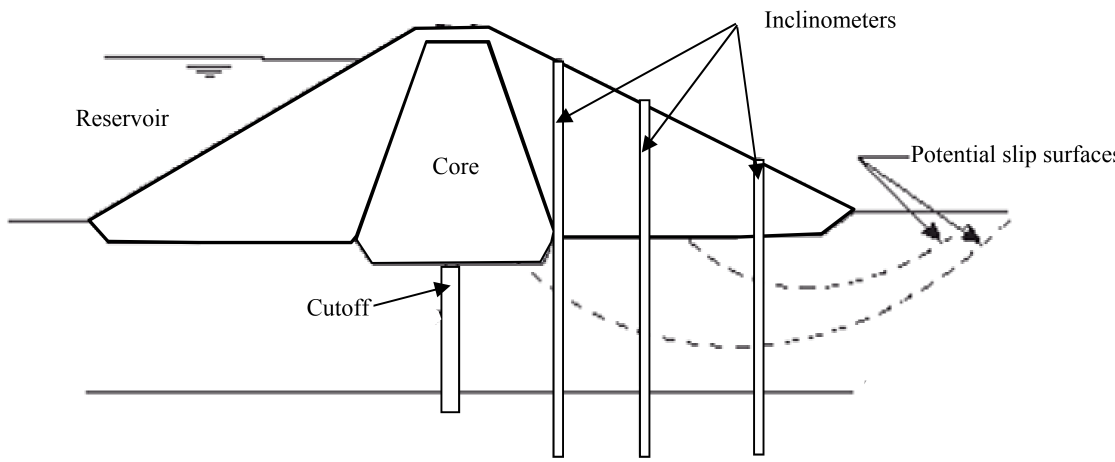

Figure 2-5:Locations for Inclinometers in Earth Dams

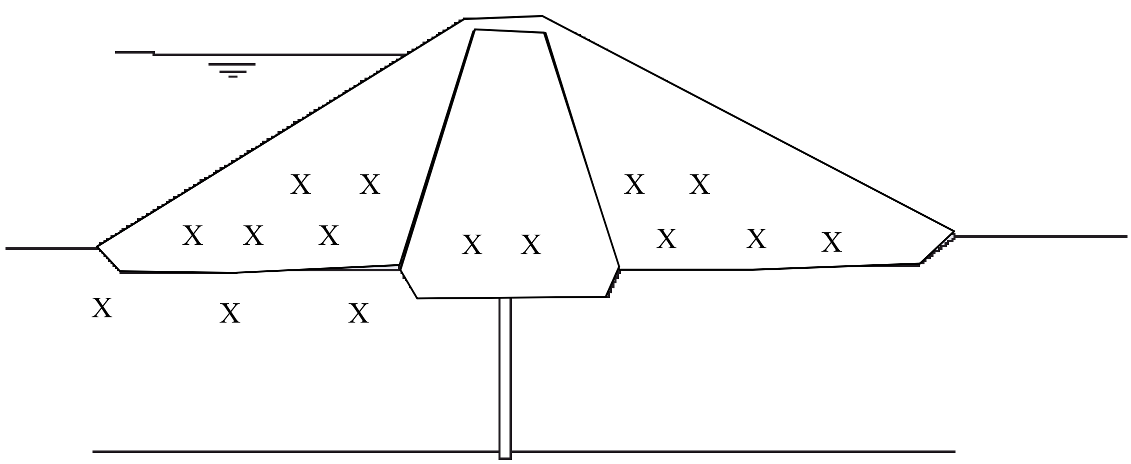

Figure 2-6:Locations for Settlement Cells in Earthfill Dams

Pressure Cells

It is used for measuring settlements and pressures in the dam body. It determines distribution, magnitude and direction of the total stress. It is located interface between foundation and dam body as shown in Figure 2-8. (DSI, 2012). Accuracy of pressure cells is ± 0.5%.

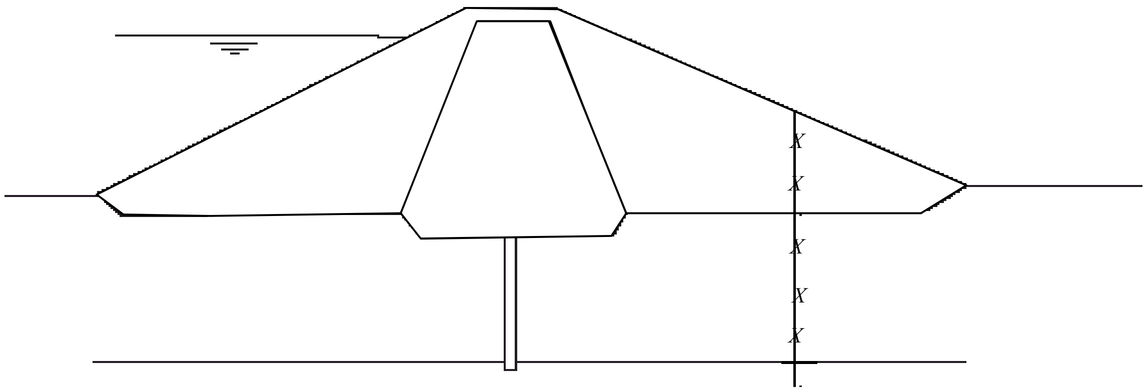

Figure 2-7:Location for Extensometers

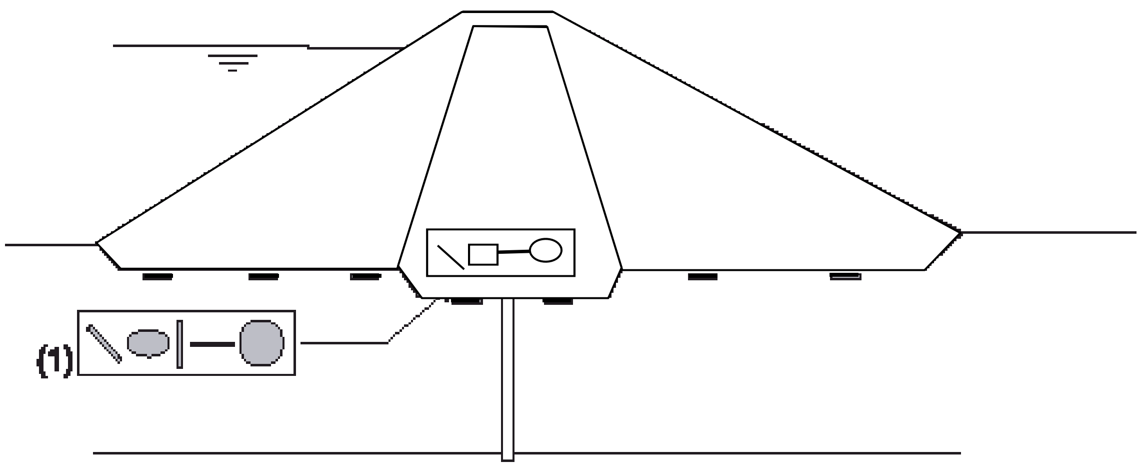

Figure 2-8:Location for Pressure cells

Drones

High-tech drones are used for detecting damages on the dam such as cracks and gate misalignments on the spillway or energy tunnels (Asctec, 2016).

Acrylamide Grout

Acrylamide monomer is produced and used as aqueous solution. While preparing the acrylamide as grout, water and other chemical are added. It includes catalyst, activators, accelerators and inhibitors. When acrylamide grout gels it becomes to impervious to water. As shown in Table 2-3, it has been used in geotechnical applications such as stopping leaks in pipes; earth, concrete dams; tunnels.

History of Acrylamide Grout

Acrylamide grout was introduced to USA in 1958 by AM-9, and it has been in USA for different purposes such as soil stabilization, leak control in pipes, concrete, earth dams and tunnels. Weidebang (2000) reported that acrylamide grout usage in USA was 43% among the other chemical grouts.

Working Properties of Acrylamide Grout

Viscosity and setting time

Tallard and Caron (1977) reported that the viscosity of acrylamide gourt is 1.2 cP at 20 C. Before it becomes gel, the viscosity of acrylamide grout doesn`t change, after becoming gel it rapidly set. Tallord and Caron (1977) offered basic test for determining gelling time for acrylamide grouts. According to this test, setting time was defined when the grout can no longer be transferred from one container to another container. AM-9 Manual (2014) reported that setting time for acrylamide grout can be controlled from 5 seconds to 10 hours.

Strength and permeability

Ozgurel (2005) reported that compressive strength of grouted sands varied from 290 kPa to 820 kPa for different size sands. Gonzalez (2005) reported that the average of friction angle of acrylamide grouted sands is 10 and cohesion is 366 kPa. Ozgurel (2005) showed that permeability of grouted sands is 10-10 cm/sec. Moreover, due to limited information about mechanical properties and permeability behavior of acrylamide grouted sands will be discussed in Chapter 4.

PH and Chemical Resistance

Uncatalyzed acrylamide grout solution has 4.5 to 5 pH (Avanti, 2014). The solution pH may affect the setting time of acrylamide grout and solution (Avanti, 2014). It should be in the range of 7 to 11. When it comes to chemical resistance, Karol (1990) showed that it has a good resistance for many chemical except for strong acids.

Table 2-3:Applications of Acrylamide Grout to Stop Water Leak.

References	Project/Location	Problems	Remarks
AM-9 Chemical Grout Manual	Indian Kill Reservoir	Heavy seepage was noted in the downstream toe after impounding.	Acrylamide grout was used to stop leaks in the dam. Soil stabilization was provided and made an impermeable barrier.
Narduzzo (2003)	Toronto Subway Tunnel	Because water level was above the tunnel, water infiltration problem occurred in the tunnel.	Total of 1,724,000 liters of acrylamide chemical grout were injected to seal 30,000 m^2 area of bored tunnel. The result was satisfied.
AM-9 Chemical Grout Manual	Tailing Dam in Argentina	Leakage Problem in the foundation.	Cement based did not prevent the leakage rate that was desired, then acrylamide grout was used. 7 years after the project was completed, there was no seepage noted in the zone.
AM-9 Chemical Grout Manual	Geehi River, Snowy Mountains, Australia	There was fissures and large voids on the rock which is located on the upper right abutment.	Permeability under dam was decreased to a adequate value.
AM-9 Chemical Grout Manual	Tsurata Dam, Kagoshima Prefecture, Japan	Seepage problem in dam body	Gel times varied from 20 to 50 minutes. Acrylamide grout reduced the permeability by a factor of 20 to as much as 100.
AM-9 Chemical Grout Manual	Oak Ridge National Laboratory	Radioactive waste leakage due to groundwater migration.	Permeability reduced to 10-8 m/sec

Seepage and Stability Analysis in Earthfill Dams

Seepage Analysis

One of the important factor for the failure of earth dams is the seepage in the body and foundation. So it is essential to control leakage inside the dam and foundation. Leakage in dams, caused water waste and, make the slope stability weak. Thus, seepage analysis is the first step and important analysis for design. According to General Directorate of State Hydraulic Works, Turkey, 2012 guidance for earth dam design book, seepage analysis can be done for two reasons. One of these is to control seepage in earthfill zone. Before slope stability analysis, phreatic surface in earthfill must be determined for rapid drawdown and state-state conditions. Second is to control seepage in foundation. The reason of this, seepage condition in the foundation must be investigated. Seepage analyses generally is done by using finite element method and software which can model flow of water. In these analyses, Darcy law is based (DSI, 2012 Guidance Book).

There are two types of seepage analysis. One of them is steady state analysis where water flow rate and water pressures do not change with time. The easiness of this analysis is that ignores the time domain and it simplifies the equations. On the other hand, in transient analysis pressure changes with time. It provides more accurate results when soil conditions are modeled, however, it is more complex than steady-state analyses.

Seepage through dam is an important task to analyze especially if dam has multiple zones. Moreover, in order to analyze seepage through dam the best method is finite element method. Using high permeability materials, having short seepage paths, cracks and fissures, and uneven settlements inside the earth dam can cause excess seepage quantity (Fattah, 2014). This discharge can be mitigated by using soils of low permeability, placing core in earth structures, cut-off in the foundations, and by increasing the seepage paths by placing upstream drains.

Kasim and Fei (2002) tried to simulate the seepage flow through an earthfill dam. In order to study seepage behavior in the dams, homogeneous and zoned earthfill dams were designed and three sets of parametric studies on long-term steady state flow were conducted. One of them was a case study, which was analysis of steady state seepage condition for Kuala Yong Dam. The calculations of seepage quantitiy of core and downstream section were made. According to results, the dischaege quantitiy changed linearly with maximum seepage velocity. Moreover after introducing hydraulic conductivity function in seepage analysis, relationship between maximum seepage velocity and flux quantity was non-linear.

Noori and Ismaeel (2009) used a finite element method software named SEEP/W to determine the quantitiy of seepage, the level of phreatic surface line, the pore water pressure distribution of Duhok dam. Moreover, the effect of the ratio of permeability in the vertical and horizontal (Kx/Ky) was investigated. Results showed that increasing Kx/Ky increased seepage quantitiy.

Seepage Theory

Seep/w which has finite element method will be used in this study. This program solves partial differential equations for 2-D steady-state and transient seepage shown in Equation 2.1 and 2.2 using finite element method.

Steady-State Analysis

$$\frac{\partial}{\partial x}\left(k_x \frac{\partial H}{\partial x}\right)+\frac{\partial}{\partial y}\left(k_y \frac{\partial H}{\partial y}\right)+Q=0\,, \tag{2.1}$$

where, kx, ky = coefficient of permeability in (x, y) directions, H= total head of water and equal to $\frac{p}{\gamma_w}+z$, P= pore water pressure, γ_w= unit weight of water, z= elevation head above sea level, Q=applied boundary flux

Transient Analysis

$$\frac{\partial}{\partial x}\left(k_x \frac{\partial H}{\partial x}\right)+\frac{\partial}{\partial y}\left(k_x \frac{\partial H}{\partial y}\right)+Q=\frac{\partial \theta}{\partial t}, \tag{2.2}$$

where, θ=volumetric water content; and t=time

The difference between two analysis is that right side has volumetric content function with time for transient analysis.

Boundary Conditions

There are four boundry conditions for unconfined seepage problems ;

1. Impervious boundry

   $$\frac{\partial H}{\partial n}=0, \tag{2.3}$$

   where, n = vertical direction of the boundry.

2. Entrance and exits: also called reservoir boundaries or submerged permeable boundaries

   H= h1 and (2.4)

   H= h2, (2.5)

   where, h1 and h2 are heads of water at entrance and exit, respectively.

3. Surface of seepage

   H= y. (2.6)

4. Line of seepage

   H= y and (2.7)

   $$\frac{\partial H}{\partial n}=0. \tag{2.8}$$

Stability Analysis

A factor of safety is used to evaluate the stability of the dam. The factor of safety is

$$FS = \frac{\tau_f}{\tau}, \tag{2.9}$$

where, FS = Factor of Safety τ_f =failure shear strength of the soil τ=shear stress of the soil.

There are two methods for stability analyses. One of them is limit equilibrium methods. This method utilizes the Mohr-Coulomb expression to determine the shear strength τ_f along the sliding surface. There are several methods developed for stability analysis. The first method was introduced by Fellenius (1936), attributed to the ordinary method of slices known as Swedish method. Bishop (1955) advanced this method introducing base normal force that interslice forces are horizontal. This method satisfies only moment equilibrium consider normal forces but not shear between the slices. Later, Morgenstern-Price (1965), Spencer (1967), Sarma (1973) made further contributions with different assumptions for the interslice forces. Montenster-Price (1965) method satisfies both force and moment equilibrium. Other method is Finite element method which is applicable for more conditions and is able to get informations about the soil movements, strains, and stresses.

Fellenius (Swedish) Method

The factor of safety for steady state seepage condition can be calculated as follows:

$$FS = \frac{\sum_{i=1}^{n} c`L_i + (W_i \cos a_i - u_i L_i) \tan \varphi`}{\sum_{i=1}^{n} W_i \sin a_i}. \tag{2.10}$$

Simplified Bishop Method

$$FS = \frac{\sum_{i=1}^{n} (c`b_i + (W_i - u_i b_i) \tan \varphi`) \frac{1}{m_{ai}}}{\sum_{i=1}^{n} w_i \sin a_i}, \tag{2.11}$$

where, $m_{ai} = \cos a_i + \frac{\tan \varphi \sin a_i}{FS}$

c`=effective soil cohesion

L= Length of the bottom of the slice,

b=width of the slice and equal to (L cosa)

u=pore water pressure

W=weight of the slice,

a= inclination of the bottom of the slice

φ =effective friction angle

Summary

Based on literature review following observations are advanced:

(1) Number of earth dams are quite high and many of them were constructed before 1986. Water leaks are big problem for these dams due to their ages. Because of internal erosion risk, they are needed to be rehabilitated.

(2) Current instruments to monitor earth dam can be damaged by consolidation of soil during construction of earth dam. Measurements from these instruments can mislead experts after construction.

(3) To simulate real condition in earth dams in terms of seepage, transient analysis is required for dam stability.

(4) Acrylamide grout has been used in geotechnical applications for decades to control water leaks, however, better characterization is needed. Performance of acrylamide grout must be investigated and documented.

CHAPTER 3 MATERIALS AND METHODS

Introduction

Acrylamide based grouts which have low viscosities, setting time, and adequate strength can be defined as an ideal grout (Karol, 1990). Because initial viscosity close to water and they can be penetrated into soil with permeability coefficient as low as 10^{-4} cm/s (Karol, 1990). They have been used in many applications such as stopping leaks in sewer systems, preventing water in tunnels, dams and other underground structures, and usage of these grouts date back 1950s (Ozgurel, 2005). Not only, acrylamide based grouts create an impermeable layer but also provide a soil stabilization. There are some cases that it was used in dams and tunnels. One of examples is Toronto Subway Tunnel which is one of the largest public transportation systems in North America. the problem in this tunnel was that groundwater level was above the tunnel roof. So, around 1,724,000 liters of acrylamide chemical grout was used to seal water leaks in the tunnel. Narduzzo (2003) reported the successful usage of acrylamide grout in this application.

This chapter summarizes the materials used and the testing methods to investigate mechanical, permeability and piezoresistivity behavior of acrylamide grouted sand.

Materials

Acrylamide Grout

In this study AV-100 (Avanti Grout International, Texas) which is commercially available grout and having the same viscosity as water was used. It is a water soluable grout and blend of acrylamide monomer with methylene bisacrylmide. In order to obtain grout solution, catalysts and activators are used. The activator called triethanolamine (TEA) which was a viscous colorless liquid starts the polymerization reaction of the chemical grout (Avanti, 2013). It is added to the grout tank containing AV-100 solution. When it is blended with ethylene glycol, it reduces its freezing temperature from 70 F to 0 F. (Avanti, 2013). The catalyst called ammonium persulfate was a white crystalline powder and is finer than AV-100. It is an initiator that triggers the polymerization reaction (Avanti, 2013). It is added to the catalyst solution. There are some chemicals that can improve some properties of acrylamide grouts. They can be summarized as follows:

1. AV-105 Ethlene glycol: It used for protecting aginst freezing and dehydration.
2. AV-257 Icoset: It is used for increasing tensile and compressive strength.
3. Potassium Ferricyanide (KFe): It is used for extending gelling time.

Sand

Commercially available silica sand was used to obtain grouted sand specimens. Four different sands were used and named as S.1, S.2, S.3, S.4. Moreover, they were characterized based on their particle size distribution. The experimental results of particle size distribution tests are summarized in Table 3-1. Typical grain size distribution for the sand is shown in Figure 3-1.

Table 3-1:Summary of Sand Properties

Selected Sand Properties				
	S.1	S.2	S.3	S.4
d10 (mm)	0.8	0.63	0.29	0.1
d30 (mm)	1.3	0.65	0.42	0.2
d50 (mm)	2.01	0.66	0.61	0.27
d60 (mm)	2.36	0.7	0.65	0.3
d90 (mm)	4	0.9	1	0.42
Cu	2.95	1.11	2.24	3.00
Cc	0.9	0.96	0.93	1.33
USCS	SP	SP	SP	SP
Remarks	Largest Sand Particles	Uniform sand particles	Medium Sand Particles	Fine Sand Particles

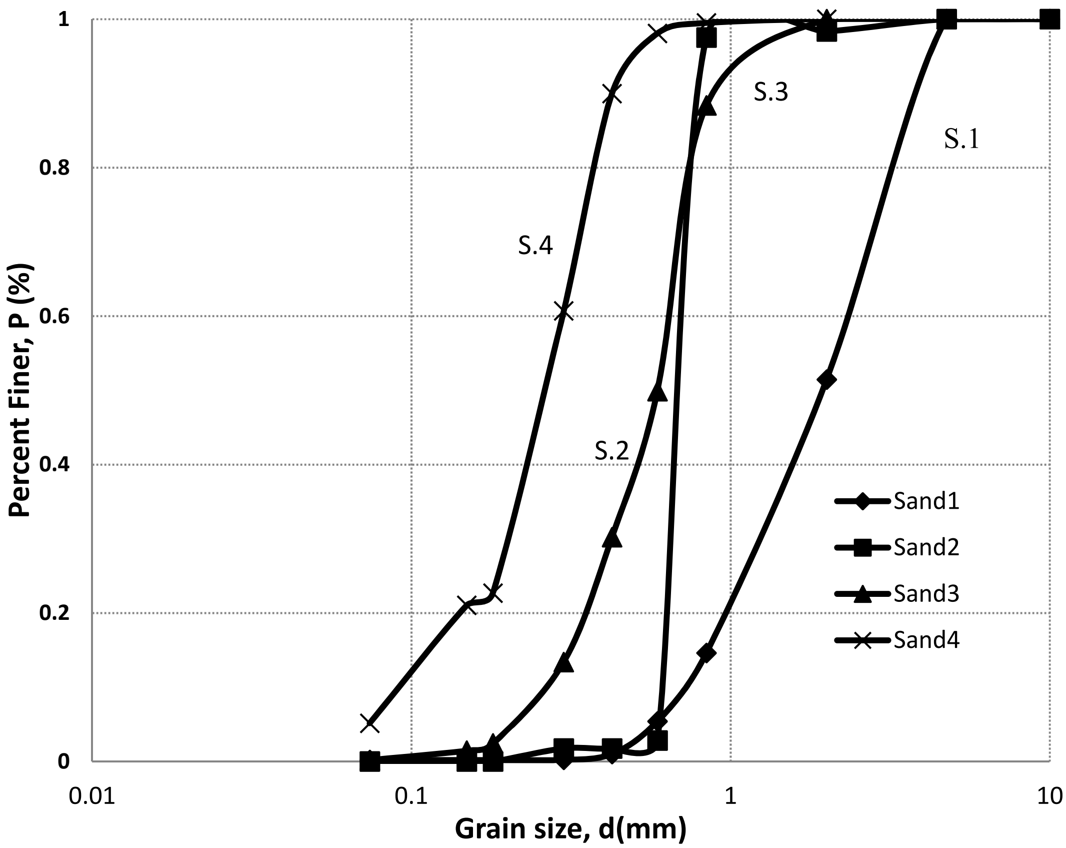

Figure 3-1:Particle Size Distribution of the Selected Sand

Specimen Preparation and Testing Method

Preparing Grout Solution

Since Acrylamide grout had two components of aqueous solution, two tanks were prepared. One tank was an aqueous solution of AV-100 and the activator which is AV-101, whereas the other was an aqueous solution of the catalyst. The amount of AV-100 was 10% by weight of the total solution. Catalyst and activator amount was kept same amount. 0.5% of catalyst and activator was used to obtain grout solution. Playing with the amount of catalyst and activator, setting time can be arranged for desired time. After preparing two tanks, they were mixed together and poured to chamber for grouting with air pressure. The mixing procedure is shown in Figure 3-2.

Tank A		Tank B		Aqueous Grout Solution
Aqueous solution 10% AV-100 0.5% AV-101	+	Aqueous solution 0.5% AV-102	=	

Figure 3-2:Mixing Procedure for Acrylamide Grout.

Grouted Sand Samples Preparation

All the grouted sand specimens were prepared in split cylindrical Teflon molds 10.2 cm (4 in.) in length and 3.8 cm (1.5 in.) in diameter. In order to keep the sand in the mold, Teflon filters were used at the bottom and top of the molds. Moreover, preventing grout leakage inside the split molds was challenged. For this problem, silicon was applied to inside and outside of the molds. The grouting apparatus has shown in Figure 3-3. It has a hydraulic system for injecting the grout from chamber into the molds and split cylinder molds. Conductive fillers were added into soil before grouting. Three specimens were prepared for each set. The dense samples were compacted with 15 hammer blows and the loose sand specimens were prepared without compaction just by pouring sand into the molds.

Grout solution was injected from bottom to up around 1 min. under 1 psi. To obtain fully grouted sand specimens, grout was allowed to flow through the column until no airbuble occurred from the top of the mold. The unit weight for dense and loose sand grouted sands was summarized in Table 3-2.

Test Methods

Permeability Test

Nine grouted sand named S.1, S.2 and S.4 were used for constant head permeability test according to CIGMAT Standart GR7-02 (Standard Test for Permeability of Grouts and Grouted

Sands). The molds were not splitted due to leakage problem. The total hydraulic gradient of 138 in. was applied over a period of 60 days. Test were performed at room condition.

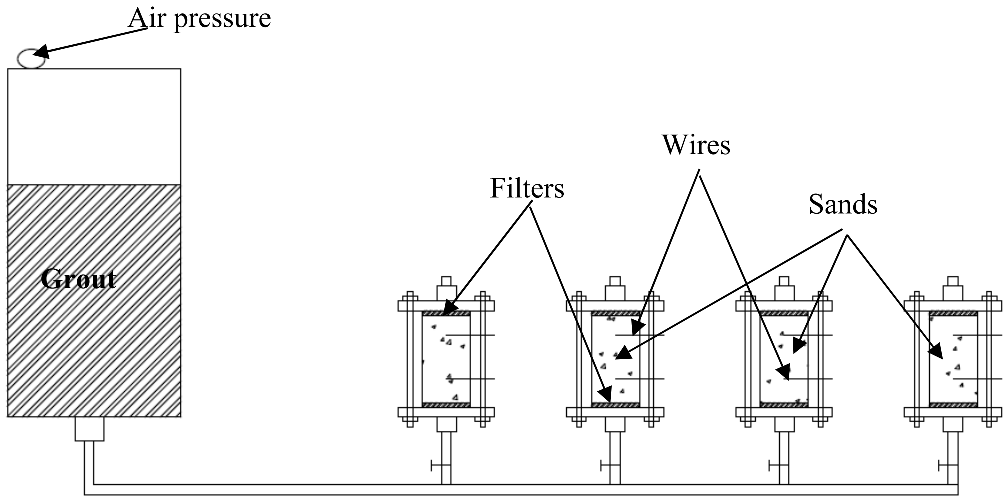

Figure 3-3:Setup for Preparing Grouted Sands

Table 3-2:Unit weight and Strength of Grouted Sand Specimens

S.1		Ottawa 20/30		S.3		S.4	
Unit Weight (g/cm^3)	Strength (kPa)	Unit Weight (g/cm^3)	Strength (kPa)	Unit Weight (g/cm^3)	Strength (kPa)	Unit Weight (g/cm^3)	Strength (kPa)
1.96	179	2.02	351	2.02	351	2	551
2.05	296	2.05	379	2.08	379	2.05	675

Unconfined Compression Tests

According to CIGMAT Standard GR02-00 (Standard Test Method for Measuring Compressive Strength of Grouts and Grouted Sands), Unconfined compression tests were performed. To obtain parallel and smooth surfaces, sulfur was applied to grouted sand specimens at the top and bottom. Samples were loaded at a strain rate of 1%/min. The machine that was used for compression tests was screw-type machine with capacity of 5,000 lbs. Specimens were tested in 3, 7, and 28 days of curing.

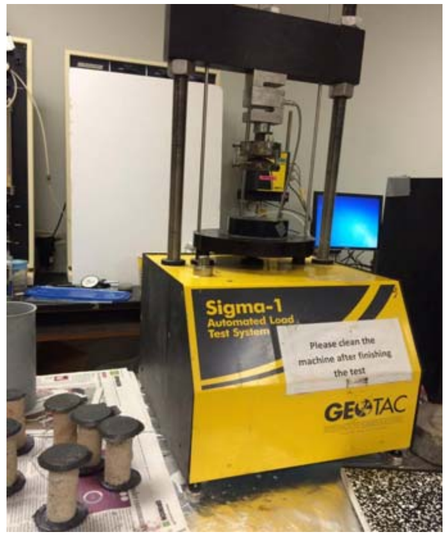

Figure 3-4:Compression Test Machine and Grouted Sand Samples

Curing Conditions

Fine grouted sand specimen was used to investigate the effect of curing condition on the mechanical properties of grouted sand. Three specimens were prepared for each set and cured at relative humidity of 50±5 % and room temperature of 23±2. Three curing condition were investigated such as by keeping them in Ziploc bags, by leaving them in the air and by placing in containers filled with water.

Gelling time

Gelling time was defined when there is no flow in the grout. In order to determine setting time, the grout mix was placed in a cup and the cup was tilted to 45. When there is no movement in the grout, that time was determined as a setting time. Sunder (2012) developed a model that estimates gelling time in his PhD thesis and CIGMAT 8-09 has given this procedure.

Water absorption

According to CIGMAT GR 3-00 standard procedure, water absorption properties were investigated for grouted sand specimens. Specimens were submerged in containers and weight change with time was observed for one week.

Piezoresistivity Test

Piezoresistivity means that the change in electrical resistivity under mechanical forces. In this study acrylamide grouted sand will be investigated and characterized. Piezoresistivity of acrylamide grouted sand was investigated under compressive loading with 0.1% Conductive filler by the weight of the sand for submerged and moist cured conditions. During the compression test, electrical resistance was obtained using LCR meter at frequency of 300 kHz (Vipulanandan et al., 2013). LCR meter is shown in Figure 3-5.

Figure 3-5:LCR Meter for Piezoresistivity Measurements

Modeling

Stress-Strain Model

In order to predict the behavior of acrylamide grouted sands for stress-strain relationship, A two parameter Vipulanandan p-q model (Vipulanandan, 1986) was used. The model is defined as shown in Equation 3.1.

$$\sigma = \left[\frac{\frac{\varepsilon}{\varepsilon_c}}{q + (1-p-q)\frac{\varepsilon}{\varepsilon_c} + p\left(\frac{\varepsilon}{\varepsilon_c}\right)^{\frac{(p+q)}{p}}} \right] \sigma_C, \qquad \textbf{(3.1)}$$

where, p and q are the material parameters, σ_c and ε_c defines the peak stress and strain. Parameter "q" represents as the ratio of secant modulus to initial modulus. P represents the optimization parameter which is calculated by minimizing the error in estimating the relationship curve. Moreover, the equation is valid by providing 0<q<1and (p+q)/q ≥ 0.

Piezoresistivity Model

In order to predict piezoresitivity behavior of acrylamide grouted sand, Vipulanandan p-q model (Vipulanandan, 1986) can be used. The model is defined in Equation 3.2.

$$\sigma = \frac{\sigma_{\max} x \left(\frac{\left(\frac{\Delta\rho}{\rho}\right)}{\left(\frac{\Delta\rho}{\rho}\right)_0} \right)}{q_2 + (1 - p_2 - q_2) x \left(\frac{\left(\frac{\Delta\rho}{\rho}\right)}{\left(\frac{\Delta\rho}{\rho}\right)_0} \right) + p_2 x \left(\frac{\left(\frac{\Delta\rho}{\rho}\right)}{\left(\frac{\Delta\rho}{\rho}\right)_0} \right)^{\left(\frac{p_2+q_2}{p_2}\right)}}, \tag{3.2}$$

where, $\sigma_{\max}$ represents the maximum stress at failure, $\left(\frac{\Delta\rho}{\rho}\right)_0$ is the piezoresistivity of the acrylamide grouted sand under peak stress, $\left(\frac{\Delta\rho}{\rho}\right)$ is the piezoresisvity at any stress and p_2 and q_2 are material parameters.

Summary

Based on literature review following observations are advanced:

1- Mechanical behavior of acrylamide grouted sand was investigated under different curing conditions. Effect of sand gradation and type on mechanical and permeability behavior of grouted sands will be investigated.

2- AC measurements was performed with 300 kHz using LCR meter to measure the electrical resistance.

3- Conductive filler was added to increase the piezoresistivity of acrylamide grouted sands.

4- The proposed Vipulanandan p-q model was used for piezoresistivity and stress-strain relationship of grouted sands.

CHAPTER 4 GROUTED SAND BEHAVIOR

Permeability of Grouted Sands

Nine grouted sand samples using S.1, S.2 and S.4 sands were used for constant head permeability tests over period of 60 days with total hydraulic head of 138 in. Whereas, before grouting the permeability of sands was 10^{-4} m/sec, after grouting grouted sands permeability reduced to 10^{-12} m/sec. Gradation of the sands and the different particle size did not affect the permeability of grouted sand. Permeabilities of sand and grouted sand is shown in Figure 4-1.

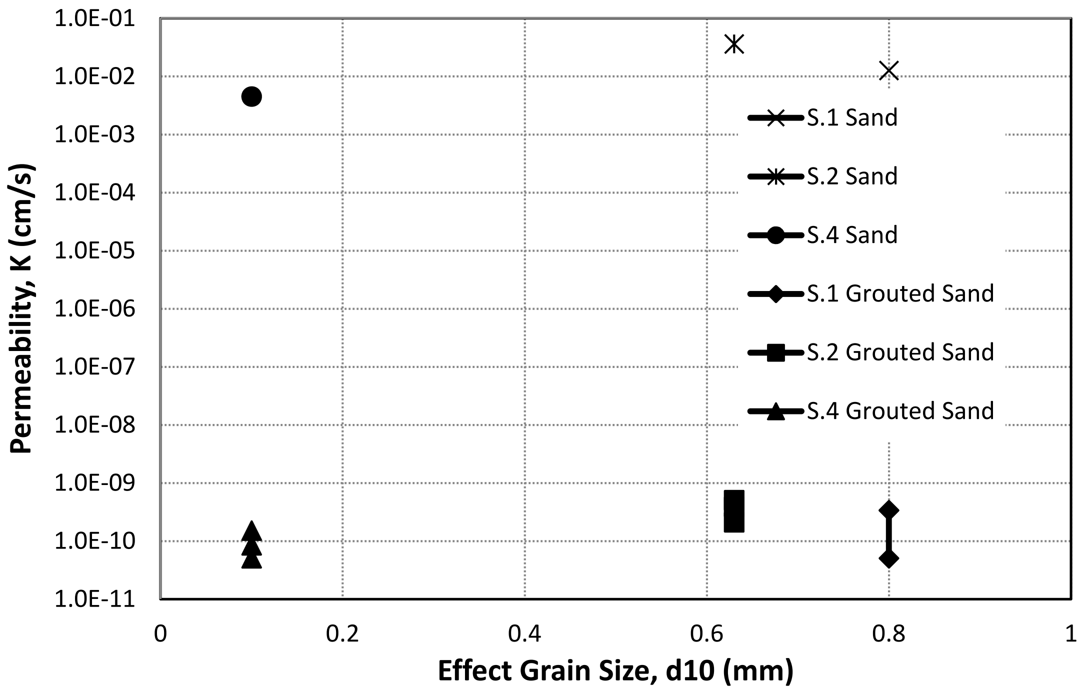

Figure 4-1:The effect of D_{10} on the Permeability of Sands and Grouted Sands

Mechanical Properties of Grouted Sand

Curing Conditions on the Mechanical Behaviour

Sample was the finest sand used to investigate the effect of curing condition on the mechanical properties of acrylamide grouted sands. The sample in water for twenty-eight days reduced the compressive strength of grouted sands. Compressive strength of grouted sand cured in air at room condition was 525 kPa. The water cured grouted sand compressive strength was 435 kPa, %17 reduction compared to air was obtained. Moist cured specimens compressive strength was 690 kPa, %58 higher compared to water cured specimens. Weight change for moist cured specimens was 0%. Water cured specimen weight increased due to absorption of water, 2% increase was observed. The sample in air loss the weight and reduction was 1.5%. Weight and density change for different curing methods are shown in Table 4-1. Elasticity modulus of water cured specimens reduced by 18% from 55 MPa to 45 MPa after 28 days curing. The elasticity modulus of air cured specimens was 96 MPa and it was 40% higher than moist cured specimens. When it comes to failure strain, submerged curing specimens was 2.14% and it was 23% higher compared to moist cured specimens. Air cured specimens failure strain was 3.5%. The influence of curing conditions on the mechanical properties of grouted sands is shown in Figure 4-2.

Table 4-1:Weight and Density Change of Grouted Sands for Different Curing Methods.

Curing Method	Initial Weight (gr)	Volume (cm^3)	Density (gr/cm^3)	Weight after 28 days (gr)	Density after 28 days (gr/cm^3)	Weight Change (%)	Density Change (%)
Moist cured	193.2	94	2.05	193.5	2.05	0%	0%
Water Cured	194.9	94.55	2.06	196.8	2.1	2%	1.90%
Air Cured	196.6	96.04	2.06	193.65	2.01	-1.50%	-2.40%

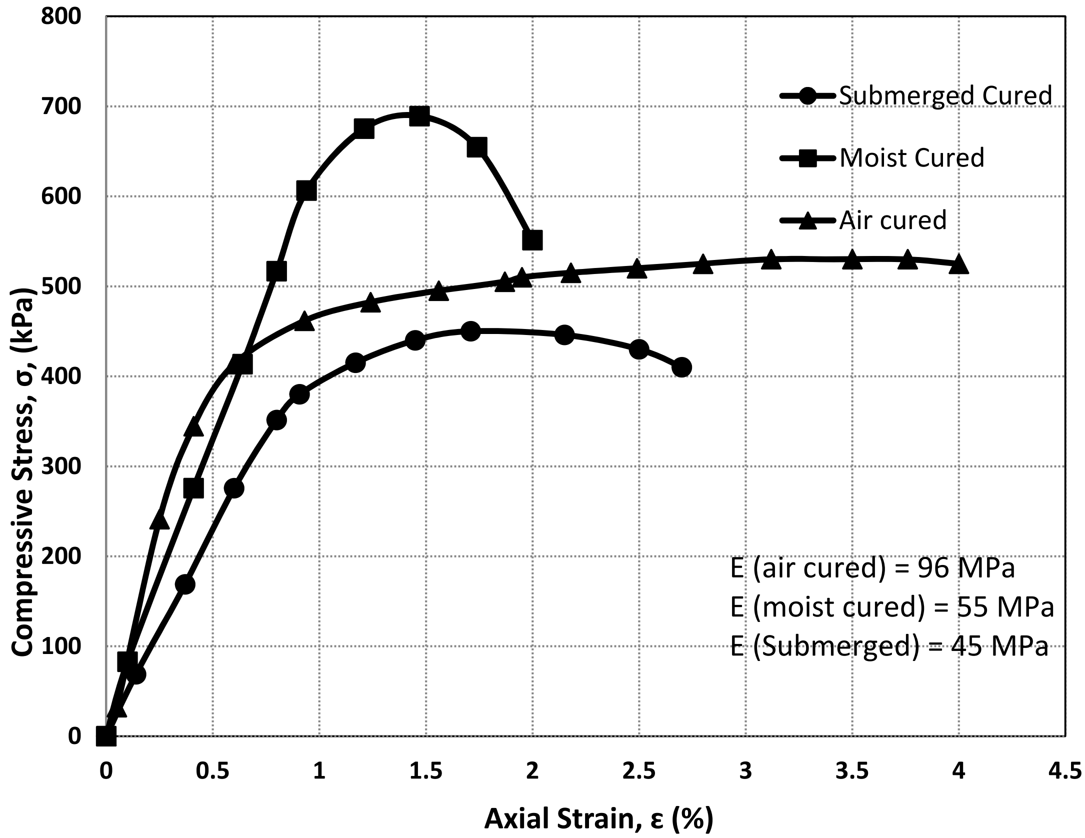

Figure 4-2:The effect of Curing Condition on the Stress-Strain relationship of Grouted Sands.

Strength

Grading of sand affected the modulus, strength and shape of the stress-strain. Decrease in particle size of the sand increased the compressive strength of grouted sands. Moreover, Figure 4-3 showed that the compressive strength was not affected after 3, 7, and 28 days curing. The compressive strength of the grouted sands varied from 240 kPa to 775 kPa. As shown in Figure 4-4, when sand was in dense state compressive strength was the highest for all type of sands. Coarsest sand named S.1 had the highest compressive strength change after compaction, 40% increase was observed. Finest sand named S.4. compressive strength was 567 kPa in loose state, then it increased up to 690 kPa. This is due to increasing in density of grouted sand. Density of the grouted sand is shown in Table 4-2. Increase in compressive strength was 18% for finest grouted sand after compaction. Stress-strain curves of seven days moist cured grouted sand specimens and model prediction are shown in Figure 4-5. Parameters for stress-strain relationship of acrylamide grouted sands are shown in Table 4-3.

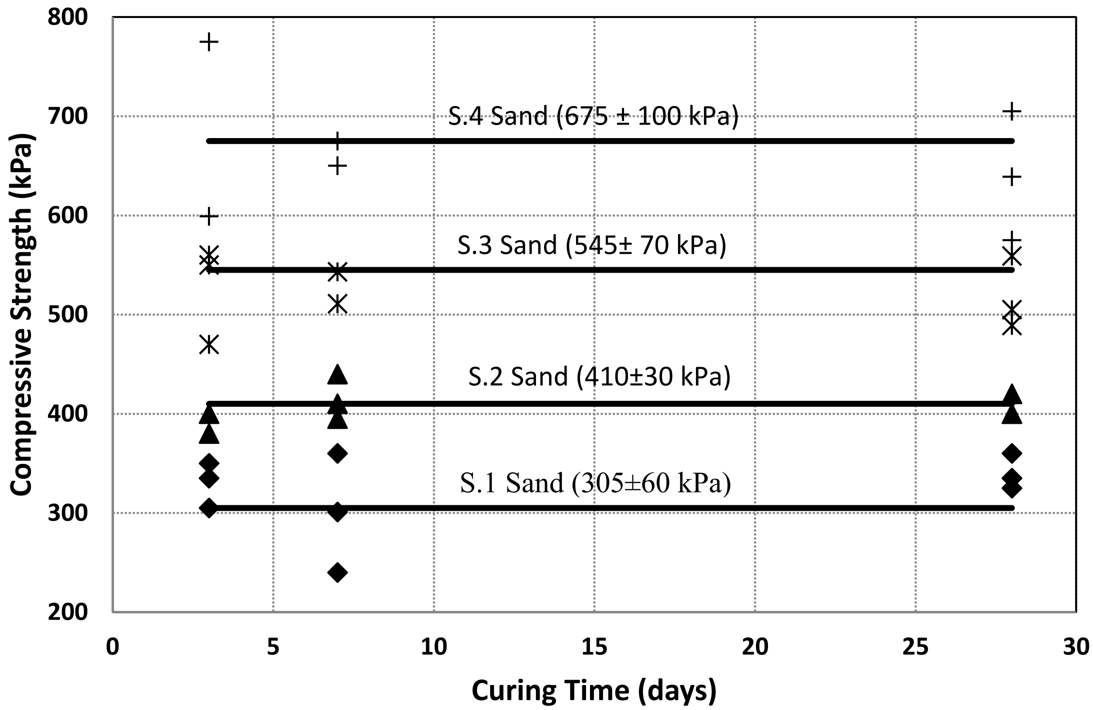

Figure 4-3:Effect of Curing Time on the Compressive Strength

Table 4-2:Density of the Acrylamide Grouted Sands

	S.1 (Coarsest sand)		Ottawa 20/30		S.3 (medium sand)		S.4 (fine sand)	
	Unit Weight (g/cm^3)	Strength (KPa)	Unit Weight (g/cm^3)	Strength (KPa)	Unit Weight (g/cm^3)	Strength (KPa)	Unit Weight (g/cm^3)	Strength (KPa)
Loose	1.96	179	2.02	351	2.02	351	2	551
Dense	2.05	296	2.05	379	2.08	379	2.05	675

Failure Strain

Whereas the failure strain was affected by the size of sand, curing time did not change the failure strain. The effect of curing time on failure strain is shown in Figure 4-6. According to results, the average failure strain varied from 1.71% to 2.25% under compacted condition. Uniform grouted sand named S.2 sand had the highest average strain failure. Average compressive failure strain of finest grouted sand named S.4 was 1.8% and it was 20% less than uniform sand. This is due to amount of grout injected. Shear type of failure was observed for many specimens, except S.1 which is coarsest sand and had cone type of failure for some specimens.

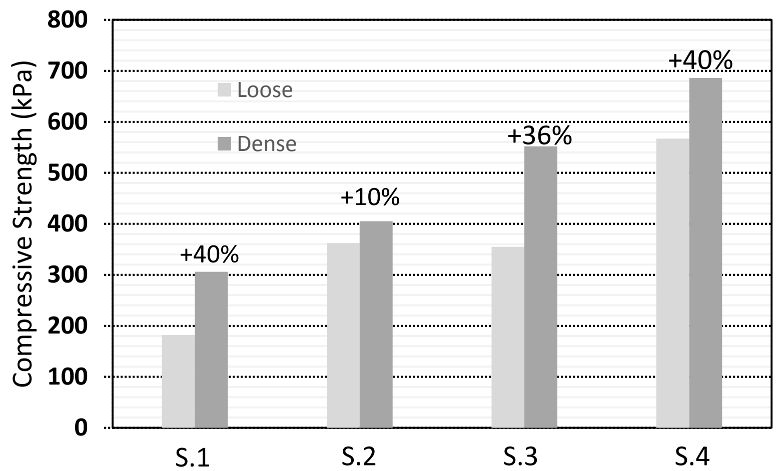

Figure 4-4:Effect of Density on the Compressive Strengths of Grouted Sand

Table 4-3:Stress-Strain Model Parameters

Sands	(p-q) Stress-Strain Model Parameters	
	p	q
S.1	0.2	0.85
S.2	0.43	0.61
S.3	0.6	0.75
S.4	0.4	0.75

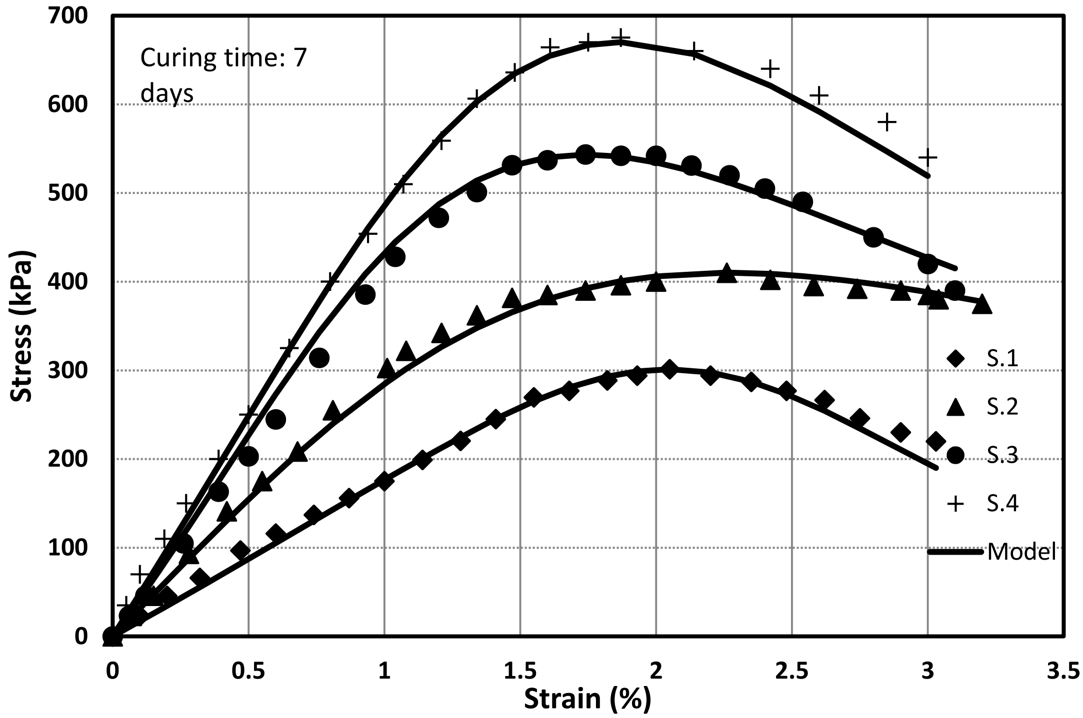

Figure 4-5:Model Prediction of Stress-Strain Behavior of Grouted Sands

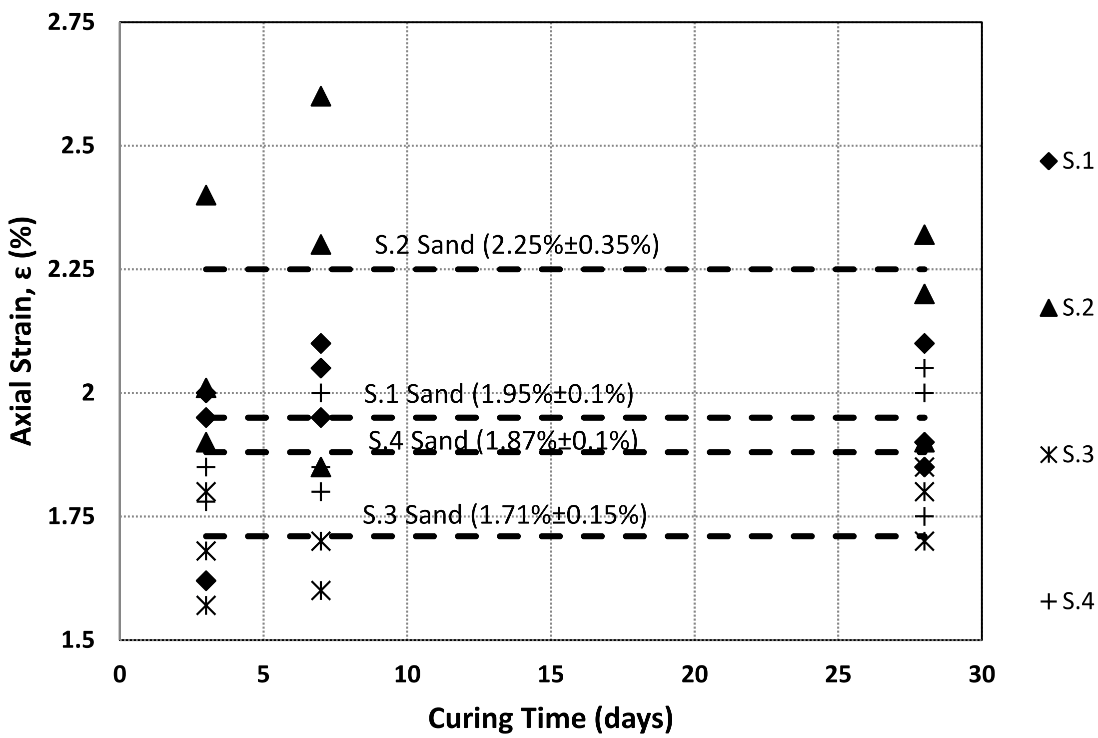

Figure 4-6:Influence of Curing Time on Strain of Grouted Sands

Modulus

As shown in Figure 4-7, Elasticity modulus of the grouted sands did not change with curing time. According to results, when the sand particle size became finer elasticity modulus of grouted sand increased. The average of grouted sand elasticity modulus was around 35 MPa for coarsest particles, whereas the fines particle modulus was about 56 MPa (S.1). It can be seen that elasticity modulus of finest particles was 138% higher than coarsest particles. Elasticity modulus of grouted sands change with effective grain size is shown in Figure 4-8. Decrease in effective grain size increased the elasticity modulus of grouted sand. As shown in Figure 4-8, elasticity modulus of finest grouted sand named S.4 was 17 MPa in loose state. However, elasticity modulus of finest grouted sand was 56 MPa after compaction. The increase in elasticity modulus was 229% for finest grouted sand. According to results, average elasticity modulus of grouted sands was 46 MPa for denser samples.

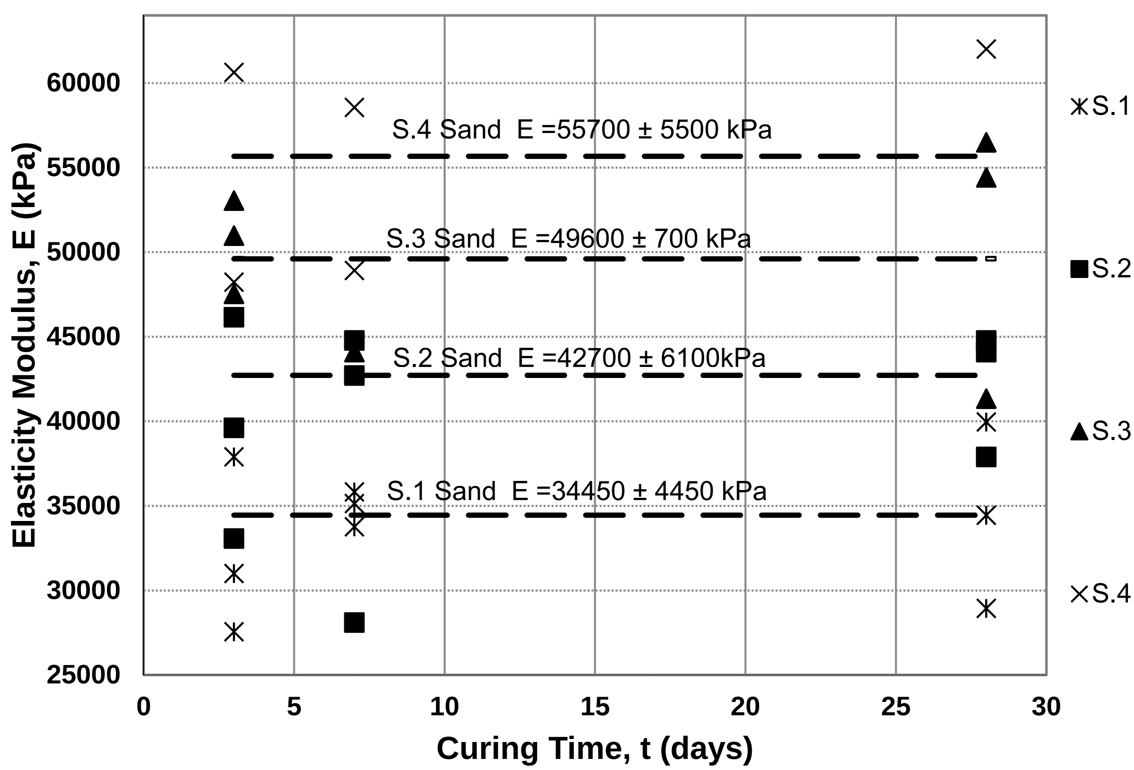

Figure 4-7:Influence of Curing Time on Modulus of Grouted Sands

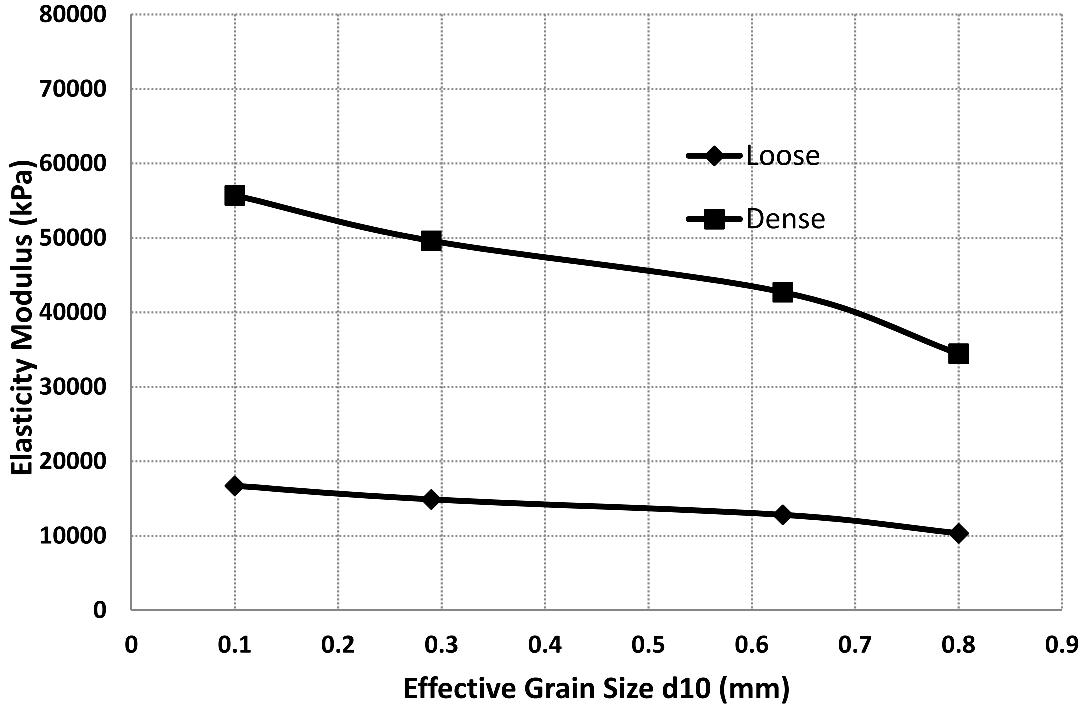

Figure 4-8:Influence of Effective Grain size on the Elasticity Modulus of Grouted Sand

Shear Strength Parameters for Acrylamide Grouted Sands

Parametric study was carried out to find shear strength parameters of the grouted sands. Shear strength parameters can be found from unconfined compressive strength values using equation (4.1). Gonzales (2005) reported that range of friction angle of the grouted sand varied from 10° to 15°. According to these values, cohesion of the grouted sands varied from 241 kPa to 325 kPa.

$$\sigma = \frac{2xCx(cos\theta)}{(1-sin\theta)}, \tag{4.1}$$

where, σ= unconfined compressive strength of the grouted sands,

C= cohesion of the grouted sands,

θ= friction angle of the grouted sands.

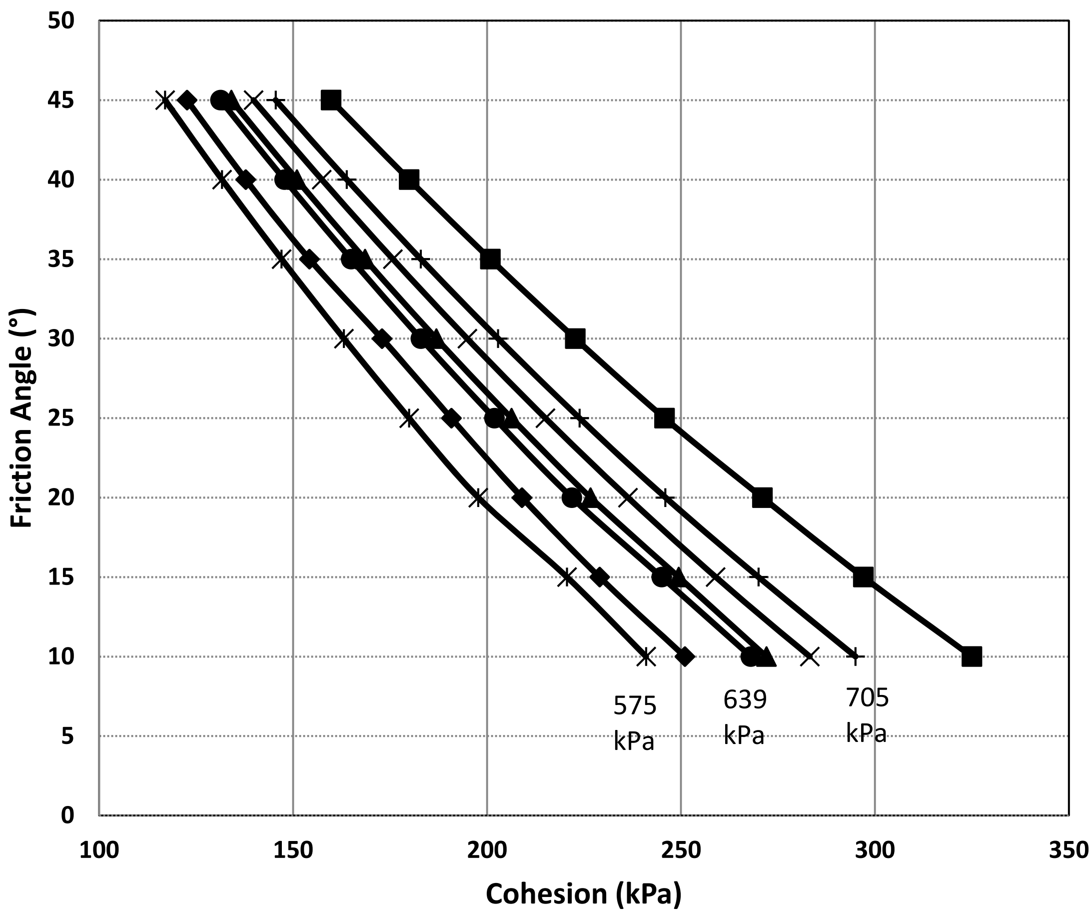

Figure 4-9:Shear Strength Parameters for Acrylamide Grouted Sands

Impedance Model

Equivalent Circuit.

It is significant to determine appropriate equivalent circuit to define the electrical properties of a material to characterize its performance with time. However, it is difficult to choose a correct equivalent circuit. Researchers adopt a circut depending on their expectation of material behavior from study to overcome this difficulty.

In this study, different possible equivalent circuits were analyzed to find a suitable equivalent circuit to represent grouted sands.

Case 1: General Bulk Material –Capacitance and Resistance

The contacts were connected in series, and both the contacts and the bulk material were represented using a capacitor and a resistor connected in parallel as shown in Figure 4.10 for Case1. In the equivalent circuit for Case 1, R_b and C_b are resistance and capacitance of the bulk material, respectively; and R_c and C_c are resistance and capacitance of the contacts, respectively. Both contacts are represented with the same resistance (R_c) and capacitance (C_c), as they are identical. Total impedance of the equivalent circuit for Case 1 (Z_1) can be represented as

$$Z_1(\sigma) = \frac{R_b(\sigma)}{1+\omega^2 R_b^2 C_b^2} + \frac{2R_c(\sigma)}{1+\omega^2 R_c^2 C_c^2} - j\left\{\frac{2\omega R_c^2 C_c(\sigma)}{1+\omega^2 R_c^2 C_c^2} + \frac{\omega R_b^2 C_b(\sigma)}{1+\omega^2 R_b^2 C_b^2}\right\}, \tag{4.2}$$

where ω is the angular frequency of the applied signal. When the frequency of the applied signal is very low, $\omega \rightarrow 0$, $Z_1 = R_b + 2R_c$, and when it is very high, $\omega \rightarrow \infty$, $Z_1 = 0$.

Case 2: Special Bulk Material - Resistance Only

Case 2 is a special case of Case 1 in which the capacitance of the bulk material (C_b) is assumed to be negligible as shown in Figure 4.11. The total impedance of the equivalent circuit for Case 2 (Z_2) is

$$Z_2(\sigma) = R_b(\sigma) + \frac{2R_c(\sigma)}{1+\omega^2 R_c^2 C_c^2} - j\,\frac{2\omega R_c^2 C_c(\sigma)}{1+\omega^2 R_c^2 C_c^2}. \tag{4.3}$$

When the frequency of the applied signal is very low, $\omega \rightarrow 0$, $Z_2 = R_b + 2R_c$, and when it is very high, $\omega \rightarrow \infty$, $Z_2 = R_b$ (**Error! Reference source not found.**).

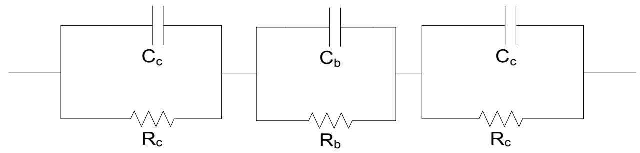

Figure 4-10:Equivalent Circuit for Case1

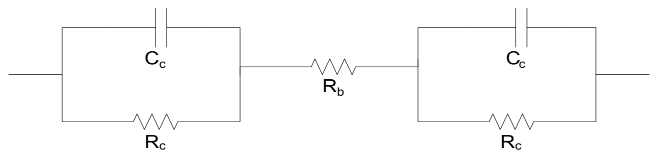

Figure 4-11:Equivalent Circuit for Case 2

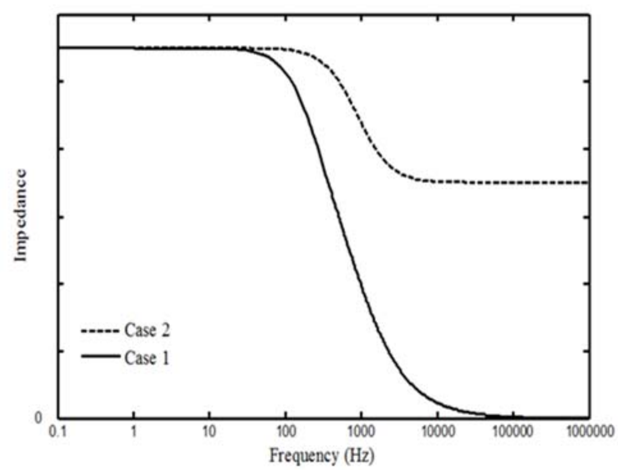

Figure 4-12:Comparison of Typical Responses of Equivalent Circuits for Case 1 and Case 2

The shape of the curves shown in **Error! Reference source not found.** is very much influenced by material response and the two probe instruments used for monitoring. Testing of grouted sand showed that Case 2 represented their behavior and hence the bulk material properties can be represented by resistivity and characterized at a frequency of 300 kHz using the two probes.

Piezoresistivity Behaviour of Grouted Sand

Piezoresistivity of grouted sand was investigated under submerged and moist cured conditions. Uniform and finest grouted sand named S.4 and S.2 were used and 0%, 0.1% CF was added to sand before grouting to investigate the effect of CF on piezoresistivity. Setting time for samples was 7 minutes. When specimens were set, resistance rapidly dropped as shown in Figure 4-13. Resistance of finest grouted sand dropped from 2130 ohm to 1810 ohm. Resistance change during setting was 15% for finest grouted sand. Initial resistance for moist cured was higher than submerged specimens. Moreover, adding CF into sand decreased the initial resistance and increased piezoresistivity behavior of acrylamide grouted sand. Piezoresistivity of uniform and finest grouted sands was similar. Initial resistance by adding 0.1% CF was 2020 ohm and it was 40% lower than 0% CF for S.4 grouted sand. Piezoresistivity of acrylamide grouted sand with 0.1% CF was 21% under 400 kPa compression and it was 50% higher compared to 0% CF acrylamide grouted sand. Piezoresistivity was 24% under 700 kPa compression for moist cured specimens with 0.1% CF. Effective grain size did not change significantly piezoresistivity. Piezoresistivity of acrylamide grouted sand for different cured conditions are shown in Figure 4-14 and Figure 4-15.

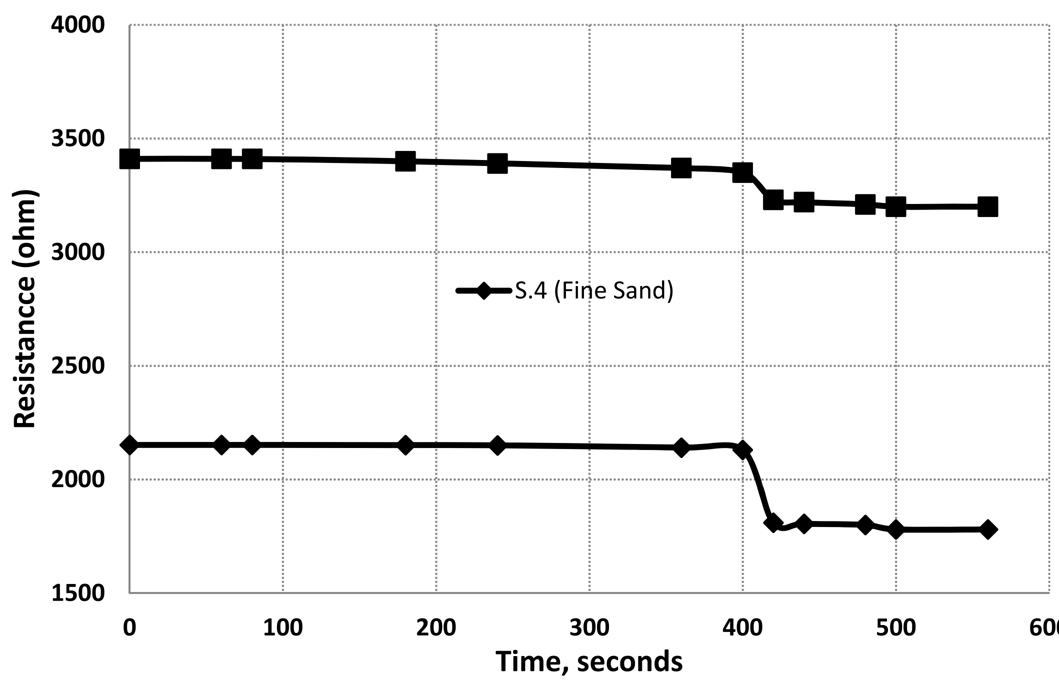

Figure 4-13:Monitoring Setting Time for Acrylamide Grouted Sands

The effect of moisture on resistivity of acrylamide grouted sand

Finest grouted sand named S.4 was used to investigate the effect of water absorption on resistivity of acrylamide grouted sand after 7 days moist cured. Firstly, specimens were cured in Ziploc bag to keep weight change zero and constant for seven days. Then, they were placed into container filled with water and left seven days. Water absorbed was similar for finest grouted sand with 0% CF and 0.1% CF. Average moisture content was 1.9% for one week. Moreover, resistivity change was observed during this time for both with and without C.F. Adding 0.1% CF into sand increased resisitivity change. Resistivity change with 0.1% CF was 13% and it was 126% higher compared to 0% CF grouted sands. Moisture effect and weight change are shown in Figure 4-16 and 4-17.

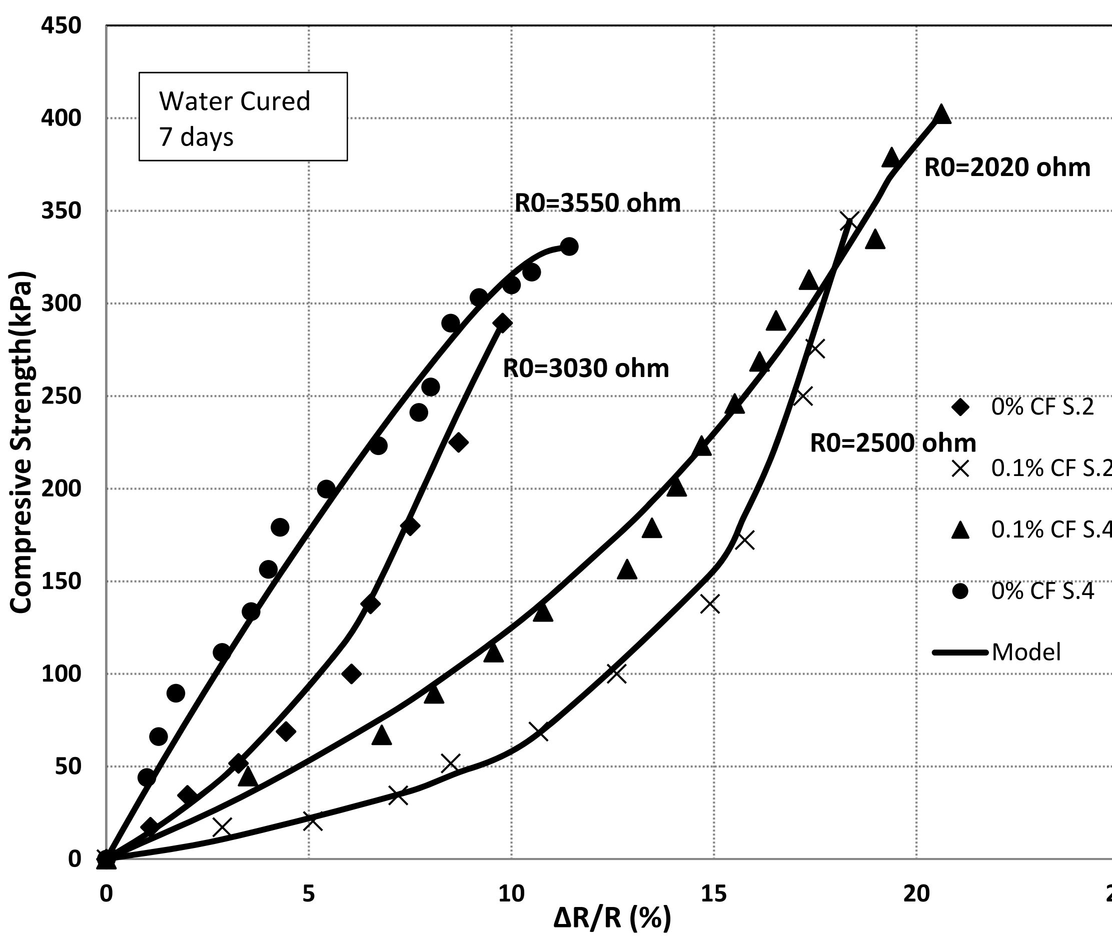

Figure 4-14:Stress-resistivity Relationship and Model Prediction of Grouted Sands

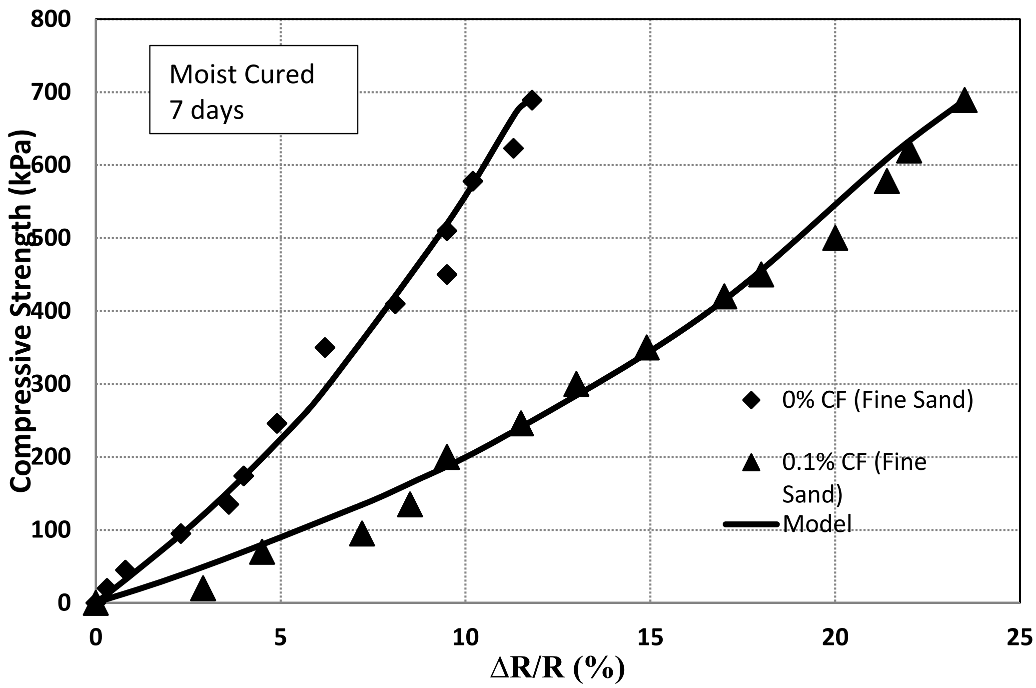

Figure 4-15: Stress-resistivity Relationship and Model Prediction of Grouted Sands

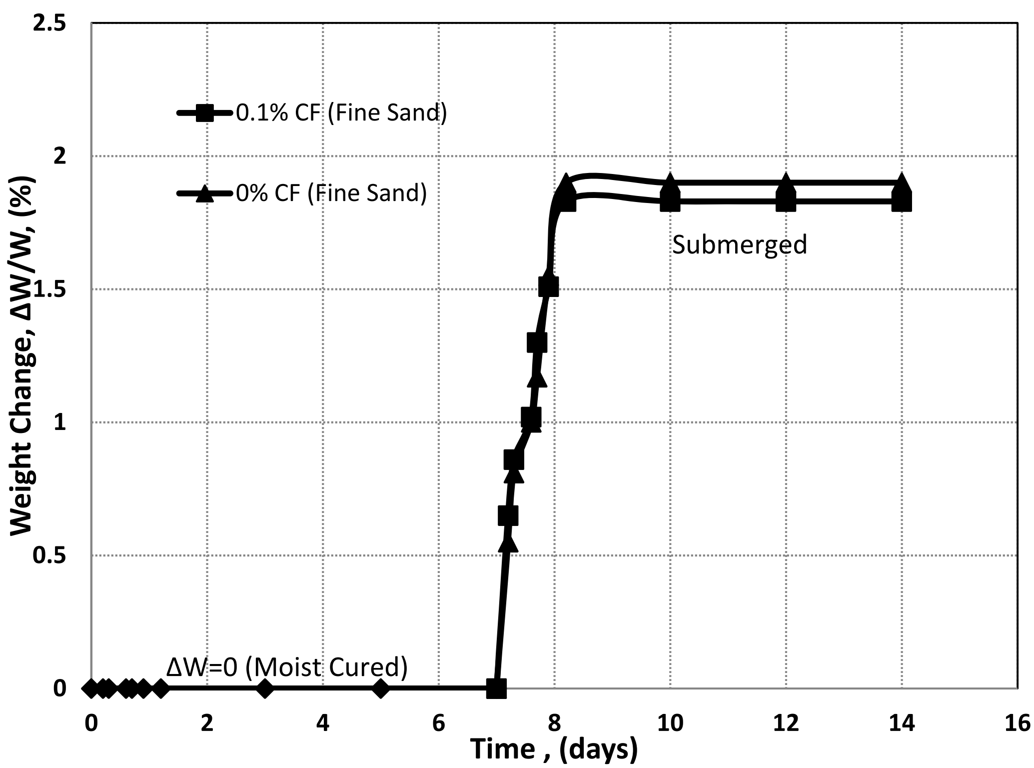

Figure 4-16:Effect of Moisture on Weight Change of Acrylamide Grouted Sand

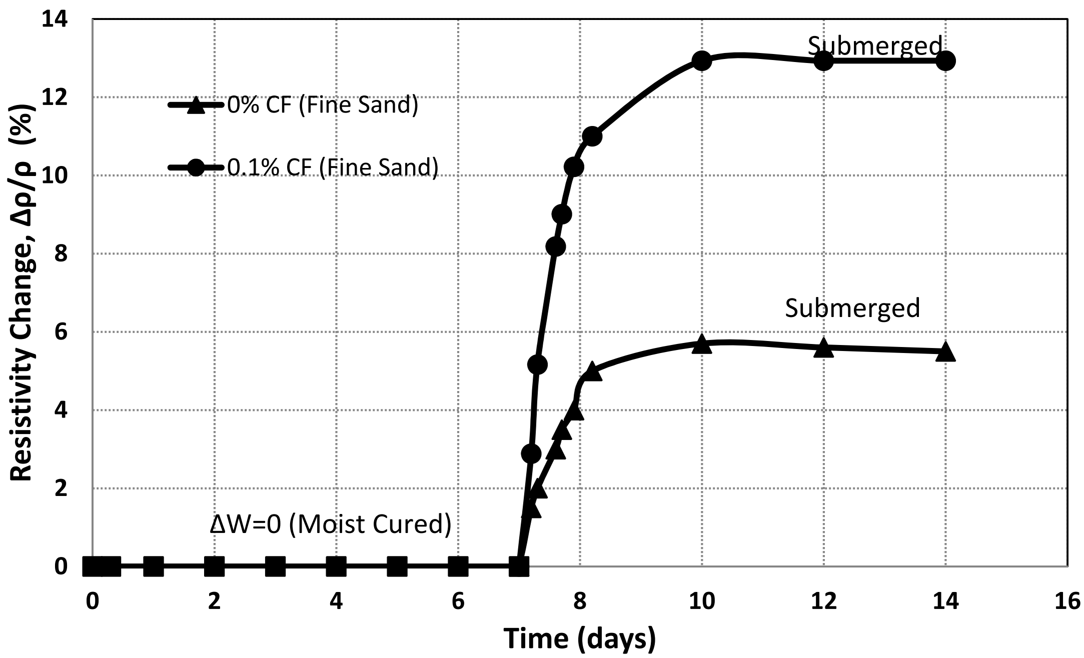

Figure 4-17:Effect of Moisture Content on Weight Change of Grouted Sand

Summary

The summary of experimental study is as follows.

1. The permeability of grouted sand was 10^{-12} m/sec, and it was not affected by grain size distribution and particle size.
2. Unconfined compressive strength was affected by the density, particle size and gradation. Strength of grouted sands increased when particles are finer. The compressive strength of the grouted sands varied from 240 kPa to 775 kPa. Moreover, curing time after 3 days did not affect the mechanical properties of grouted. P-q model can be used to predict the mechanical behavior of acrylamide grouted sands.
3. Failure strain and elasticity modulus of acrylamide grouted sands were not influenced by the curing time after 3 days. Average failure strain varied from 1.7% to 2.25% for the grouted sands for 7 days moist cured. Elastisite modulus of the grouted sands varied from 35 kPa to 56 kPa.

4. The acrylamide grouted sand with and without conductive filler were pizoresistive. Adding conductive filler into the sand increased the sensitivity of the grouted sands.The average change in resistance change at peak compressive stress was 21% for submerged specimens and 24% for moist cured specimens.

CHAPTER 5 SEEPAGE CONTROL AND MONITORING IN EARTH DAMS

Introduction

Some of the geotechnical engineering problems includes consolidation, heave, collapse and dramatic change in shear strength are directly associated with the behavior of unsaturated soils (Suhail, 2008). The stability of the embankment slope is related to its geometry, material properties and the forces acting on it (Griffith, 2000). Nowadays, numerical simulations are used to analyze stability of dams (Sakamoto T, 2002). Designers should provide an adequate factor of safety in their analysis of slope stability for their design (Suhail, 2008). This is significant to make sure that the designed slopes are safe and to prevent under critical conditions (Suhail, 2008). Table 5-1 summarizes the values of factor of safety used for earth dam design.

Earth dams may become saturated by leakage flow during a long term high reservoir level. If the reservoir pool drawdown is faster than the pore water can dissipate, excess pore water pressures can reduce the stability of the earth dam. This is called drawdown and that is common in the earth dams (USACE). One of the most severe loading conditions is rapid drawdown condition in the earth dams (Zomorodian, 2010). Rapid drawdown can bring about a temporary increase in pore water pressure and the increased seepage forces may cause to slope instability and erode the structure. Pinyol (2008) reported that the range of drawdown rate is from 0.5 to 1 m/day in dam engineering.

Table 5-1:Minimum Factor of Safety Values for Earth dams by USACE, 2003

	End of construction		Steady-state		Rapid drawdown
	Upstream	Downstream	Upstream	Downstream	Upstream
Minimum Factor of Safety	1.3	1.3	1.5	1.5	1.1

Dam Model and Material Properties

Based on five earth dams the average number dimensions was used as summarized in Table 5.2. The average slopes for upstream and downstream were 2.5H:1.0V and 2.25H:1.0V, respectively. According to these average slope of the earth dam, material types of the zones were selected from Bureau of Reclamation and summarized in Table 5-3. Soil types were SP, GP, SW or GW can be chosen for downstream, and SC or SM can be selected for core. In this study, SP was selected for upstream slope. The most important soil parameters for the stability analysis are friction angle and cohesion of the soils were chosen according to soil types from the USACE MANUAL as shown in Table 5-4. The dam configuration is shown in Figure 5-1 and material properties listed in Table 5-5.

Table 5-2:Selected Earth Dams for Model

Dam name	Purpose	Upstream Slope	Downstream Slope	Height (m)	Crest length (m)	Foundation	References
Howard Praire	Any	2.5 : 1	2.0 : 1	27	9	No information	Bureau of Reclamation
Dry falls dam	Storage	2.0 : 1	2.0 : 1	14	6	No information	
Tiber	Storage	3.0 : 1	2.5 : 1	15	8	No information	
Maneciu dam	supplying water electricity	2.5:1	2.5:1	78	12	30	Andreea (2015)
Al-adhaim da	supplying water electricity	2.5:1	2.0 : 1	43.5	12	30	Fattah (2014)
Average		2.5 : 1	2.25 : 1	35	9	30	

Table 5-3:Recommended Material Types for Zoned Earthfill Dams by Bureau of Reclamation (USBR, 1986).

Type	Purpose	Subject to rapid drawdown	Shell material Classification	Core material Classification	Upstream Slope	Downstream Slope
Zoned with maximum core	Storage	Yes	Not critical GW, GP, SW or SP	GC, GM	2.5 : 1	2.0 : 1
				SC, SM	2.5 : 1	2.25 : 1
				CL, ML	3.0 : 1	2.5 : 1
				CH, MH	3.5 : 1	3.0 : 1

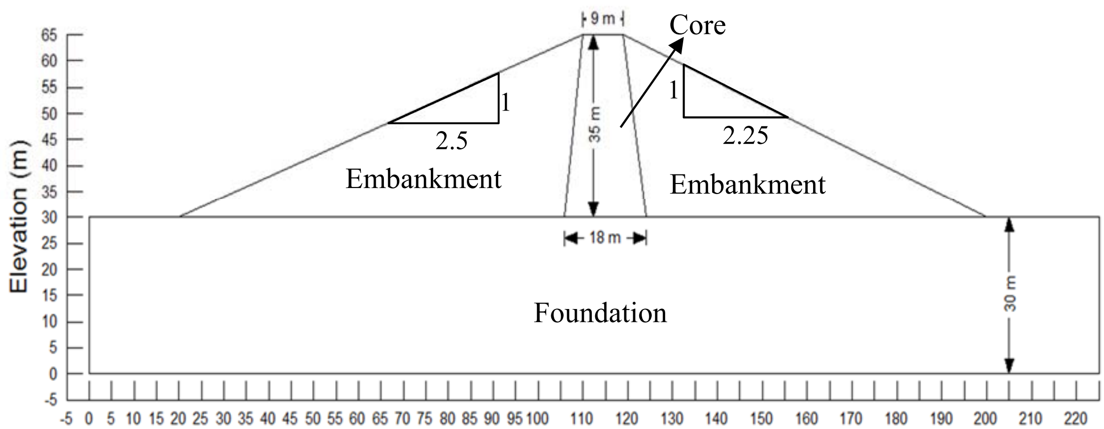

Figure 5-1:Dam Geometry

After determining the geometry and material properties, the soil volumetric characteristic curve has to be defined in the analysis of the earth dam for unsaturated conditions. Since soil volumetric water content is not available, volumetric water contents were estimated for the earth dam materials from Souliyaveong (2012) as shown in Figure 5-2.

Modeling and Analysis

The analysis was performed including transient seepage analysis to determine pore-water pressures during drawdown and stability analysis of the upstream dam slope. These two analysis were conducted in coupled mode. Each material zone was assumed homogeneous and isotropic for the analysis.

Seepage Analysis

Seep/w which has the finite element method was used to simulate 2-D steady state and transient seepage in the earth dam before and during the rapid drawdown. This software governes differential equation which is $\frac{\partial}{\partial x}\left(k_x \frac{\partial H}{\partial x}\right)+\frac{\partial}{\partial y}\left(k_x \frac{\partial H}{\partial y}\right)+Q=\frac{\partial \theta}{\partial t}$ for 2-d seepage using Finite Element.

Table 5-4:Values for Shear Strength of Soil Materials (USCS).

USCS Soil Type	Laboratory		Placement		Effective Stress		
	Max. Unit weight (lb/ft^3)	Optimum moisture content	Unit weight	Moisture content (%)	C` (kPa)	Friction angle	Values listed
SP	115.6	10.8	103.4	5.4	8.1	37.4	Average of all values
	9.7	2	14.6	-	3	2	Standart deviation
	106.5	7.8	88.8	5.4	2.5	35.4	Minimum value
	134.8	13.4	118.1	5.4	8.4	39.4	Maximum value
	7		2				Total number of test
SM	116.6	12.5	112	12.7	20.7	34	Average of all values
	8.9	3.4	11.1	5.4	25.5	4.9	Standart deviation
	92.9	6.8	91.1	1.6	0	23.7	Minimum value
	132.6	25.5	132.5	25	90.3	40.7	Maximum value
	123		17				Total number of test
SC	118.9	12.4	115.6	14.2	19.3	32.7	Average of all values
	5.9	2.3	14.1	5.7	14.5	3.8	Standart deviation
	104.3	6.7	91.1	7.5	0	25.5	Minimum value
	131.7	18.2	131.8	22.7	42.1	38.3	Maximum value
	90		11				Total number of test

Table 5-5:Material Properties for Earth Dam

Material Properties	Symbol	Unit	Values				Remarks
			Clay core	Embankment	Grouted Sand	Foundation	
Saturated hydraulic conductivity	k_{sat}	m/sec	$1x10^{-6}$- $1x10^{-10}$	$1x10^{-4}$-$1x10^{-6}$	$1x10^{-12}$	$1x10^{-7}$	embankment permeability varied 10-4to 10-6
Saturated Unit weight	γ_{sat}	kN/m^3	14.6-20.8	16.7-21	20.2-20.8	19-21.5	Unit weight varied from 14 to 21.5 for material types
Effective Cohesion	c`	kPa	10-42.1	2.5-8.4	244-325	0-5	embankment cohesion was varied from 2.5 to 8.4
Effective friction angle	ϕ	degree	25.5-38.3	35.4-39.4	10-15	30	Friction angle was varied from 25 to 39
Volumetric water content	Θ_w	m^3/m^3	0.4	0.32	0.015	0.3	values for SWCC were taken from Souliyavong, 2012
Elastisite modulus	E	Mpa	30-60	50-80	34-56	60-80	based on Obrzud & Truty (2012)
Poisson ratio	v		0.35-0.40	0.25-0.30	0.25-0.35	0.1-0.4	based on Obrzud & Truty (2012)
Remarks			Values were taken from USBR (Compacted Soils)		Lab. Tests were carried out	Fattah (2014)	

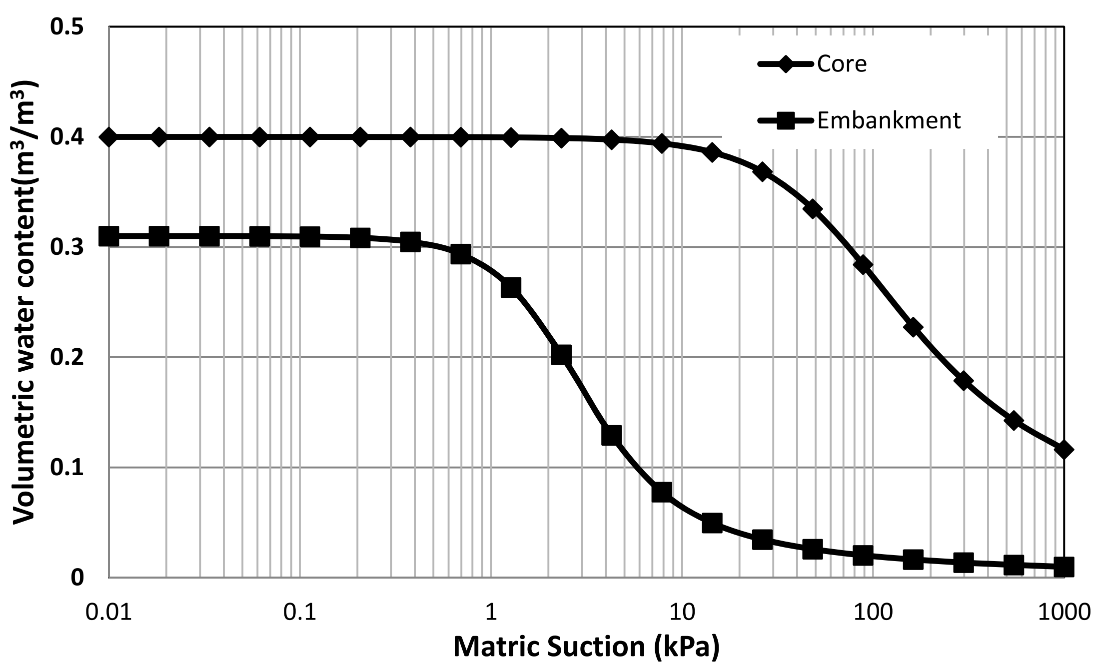

Figure 5-2:Soil Water Characteristic Curve for Unsaturated Shear Strength Parameters for Earth Materials (Souliyavong, 2012).

Finite Element Analyses

The finite element mesh shown in Figure 5.3 was used to generate the dam structure. The mesh was defined as an unstructured pattern of quadrilateral and triangular elements with 3 and 4 nodes respectively. Before drawdown condition, effect of mesh size on the seepage quantity and phreatic line was investigated under steady-state condition. Maximum element size was 5mx5m and minimum was 1mx1m. Moreover, the dam was analyzed for steady-state seepage conditions and assuming reservoir level at the dam crest (elevation 65m) which is a critical condition.

Boundary Conditions

According to SEEP/W manual, boundary conditions can be only one of two fundamental options. H (head) or Q (total flux) must be defined (SEEP/W).

There are four type boundry conditions for unconfined seepage problems ;

1. Impervious boundry

   $$\frac{\partial H}{\partial n} = 0, \tag{5.1}$$

   where, n = vertical direction of the boundry.

2. Entrance and exits: also called reservoir boundaries or submerged permeable boundaries

   H=h1= 65m and (5.2)

   H=h2= 30m, (5.3)

   where, h1 and h2 are heads of water at entrance and exit, respectively.

3. Potential Seepage Face

   H= y=30 m. (5.4)

4. Line of seepage

   H= y and (5.5)

   $$\frac{\partial H}{\partial n} = 0.$$

In this study, H (total head) was defined. The boundaries ABC and DE as shown in Figure 3 were defined as constant total head boundaries with values of 65m and 30m respectively.

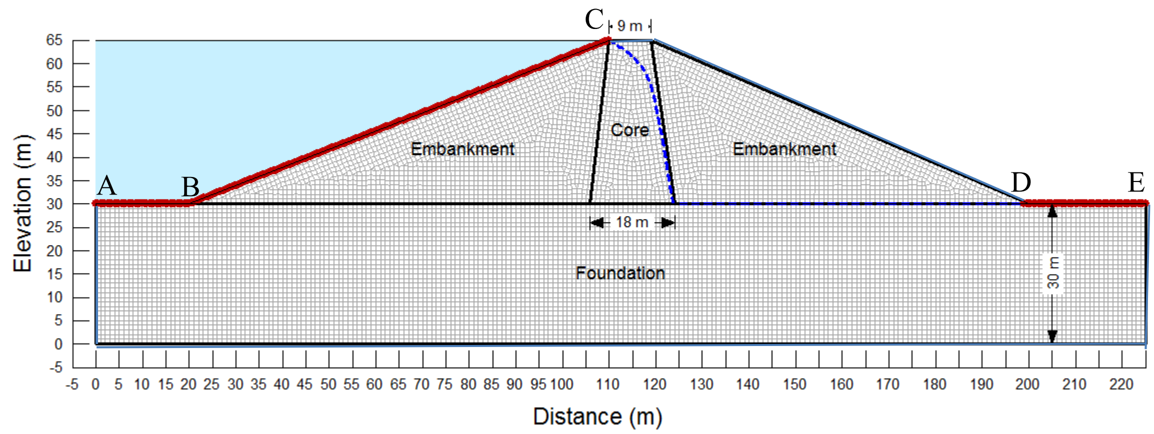

Figure 5-3:Earth Dam with Mesh and Boundary Conditions for Steady-state Analysis

The initial pore-water pressure distribution calculated from steady-state analysis was defined performing transient analysis. As shown in Figure 5.3, the upstream boundary (ABC) and (DE) condition was defined to simulate the reservoir drawdown . This boundary will provide the user to define the change in reservoir level as a function of time. The reservoir level was dropped linearly from 65m to 30m. During the drawdown, the shear strength of the materials could change from saturated to unsaturated and then the saturated hydraulic conductivity of each material should be defined as a function of suction Souliyavong (2012). Fredlund and Xing`s (1994) method was used to estimate the hydraulic conductivity function for each material. In this method, hydraulic conductivity function can be found using its Volumetric water content function and saturated hydraulic conductivity. The transient seepage analysis will give the changes of pore-water pressures with drawdown time by means of the FE mesh.

Stability Analysis

Slope/w which has limit equilibrium method was used for stability analysis of upstream slope during drawdown. Bishop method was used to evaluate minimum factor of safety. Trial failure surfaces were defined using the entry (CD) and the exit (AB) method for each scenario as shown in Figure 5-4. The Slope/w analyses most critical surface with a minimum factor of safety for each drawdown scenario is obtained from all the trial surfaces.

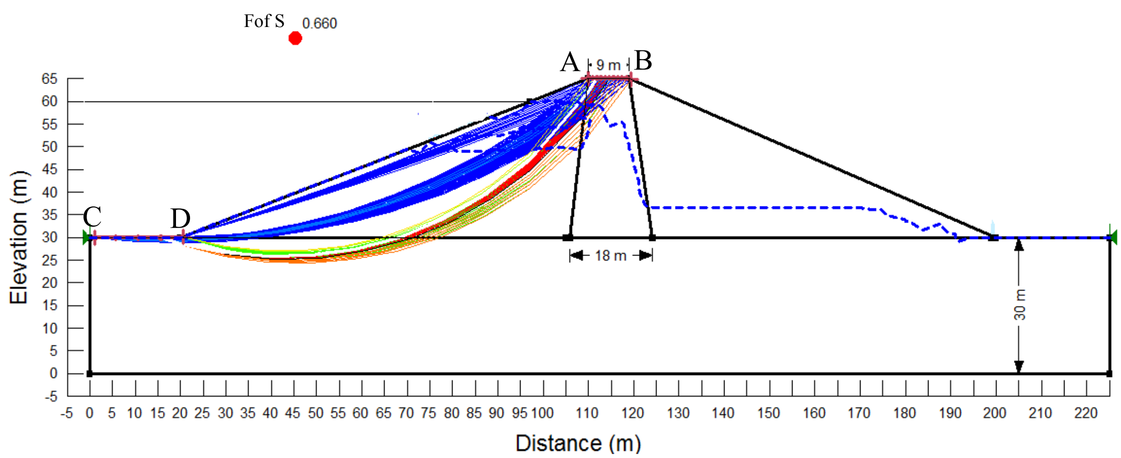

Figure 5-4:Critical Trial Surfaces for Rapid Drawdown Condition

Because the drawdown condition generates unsaturated conditions in the dam materials, the unsaturated shear strengths of the materials must be considered. In this analysis, Eq. (5.1) suggested by Vanapalli (1996) was used to estimate unsaturated shear strength of the materials.

$$\tau = c` + (\sigma_n - u_a)\tan\phi` + (u_a - u_w)\left[\left(\frac{\theta_w - \theta_r}{\theta_s - \theta_r}\right)\tan\phi`\right], \qquad (5.6)$$

where τ =shear strength of saturated/unsaturated soil ; c`=effective cohesion of saturated soil; $\sigma_n$=total normal stress on the failure plane of the soil; $\phi`$ =effective friction angle; $(u_a - u_w)$= matric suction in the failure plane of the soil; u_a=pore-air pressure in saturated soil; u_w= pore-water pressure θ_w= volumetric water content, θ_s=saturated volumetric water content, θ_r= residual volumetric water content can be estimated to be equal to 10% of θ_s .

Results and Discussions

Effect of Mesh Size on Leakage Flow Rate and Phreatic Line

Three mesh size was considered such as 5mx5m, 3mx3m and 1mx1m respectively. Node and element numbers are shown in Table 5-6. According to results, the leakage rate was affected by mesh size. When mesh size becomes finer, seepage value decreased. Seepage decreased 29% when mesh size varied from 5mx5m to 1mx1m for dam body. The change for foundation seepage was 25% which is almost similar to change in body. Phreatic line change is negligible under different mesh size in Figure 5-4. According to the results, clay which had low permeability had good resistance against water seeping into the dam and phreatic line dropped sharply as shown in Figure 5.4.

Table 5-6:Effect of Mesh Size on Seepage Quantity

Seepage location	Mesh size		
	1mx1m	3mx3m	5mx5m
Body (10^{-3} m^3/day/m)	2.6	3.1	3.7
Foundation (10^{-3} m^3/day/m)	5.6	6.1	7
Node Number	46440	5368	1996
Element Number	15261	1715	621

Effect of Slope on Miminum Factor of Safety

After analyzing earth dam with 2.5H : 1V upstream slope, earth dam was stable for both steady state and end of construction, however, minimum factor of safety for rapid drawdown condition was 0.66 which is lower than required min fof safety according to USACE Manual. Therefore, upstream slope with 3.0H:1V and 4.0H:1V was used for stability analysis to have stable earth dam. Table 5-7 shows that earth dam designed with 4.0H:1V was stable. Factor of safety values for 3.0H:1V and 4.0H:1V were 0.716 and 1.216, respectively. As shown in Figure 5-5 The

1st, 2nd, 3rd days were more critical days for rapid drawdown condition.

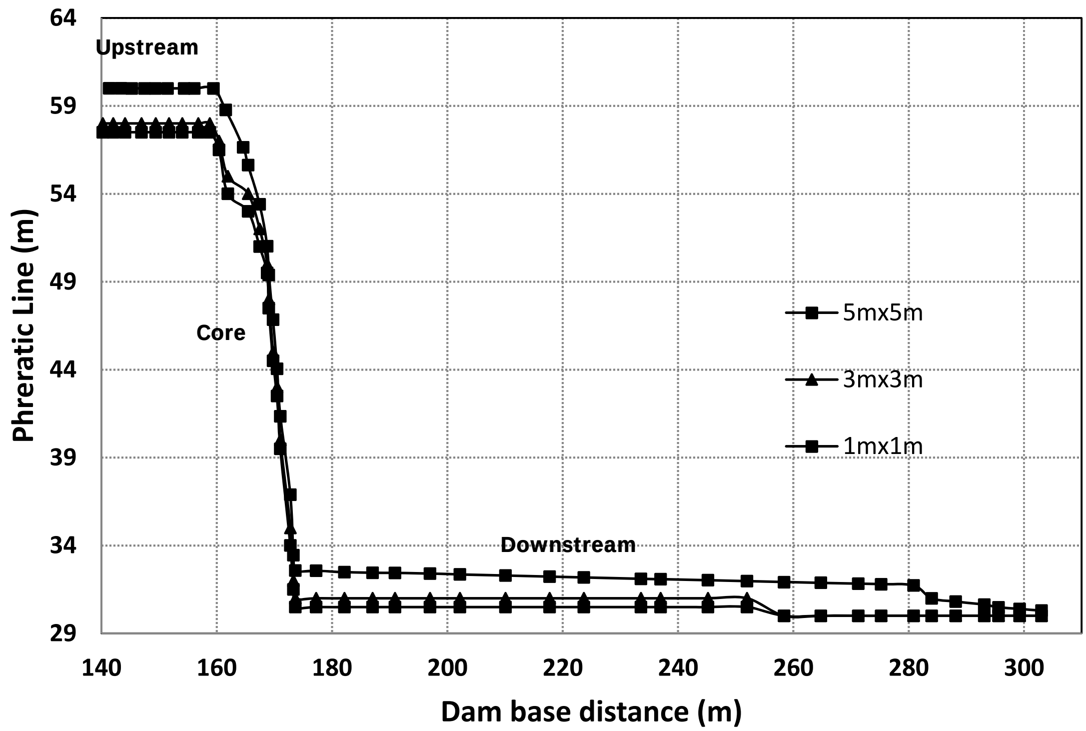

Figure 5-5:Effect of Mesh Size on Phreatic Line Level

Table 5-7:Effect of Upstream Slope on Minimum Factor of Safety Under Three Conditional.

Analysis method	Slope	End of construction		Steady-state		Rapid drawdown	Remarks
		Upstream (FofS)	Downstream (FofS)	Upstream (FofS)	Downstream (FofS)	Upstream (FofS)	
Bishop	2.5 H : 1.0 V	2.267	2.058	2.397	1.842	0.660	Failure
Bishop	3.0 H : 1.0 V	2.615	2.636	2.735	2.65	0.716	Failure
Bishop	4.0 H : 1.0 V	3.579	3.55	3.677	3.3	1.216	Stable

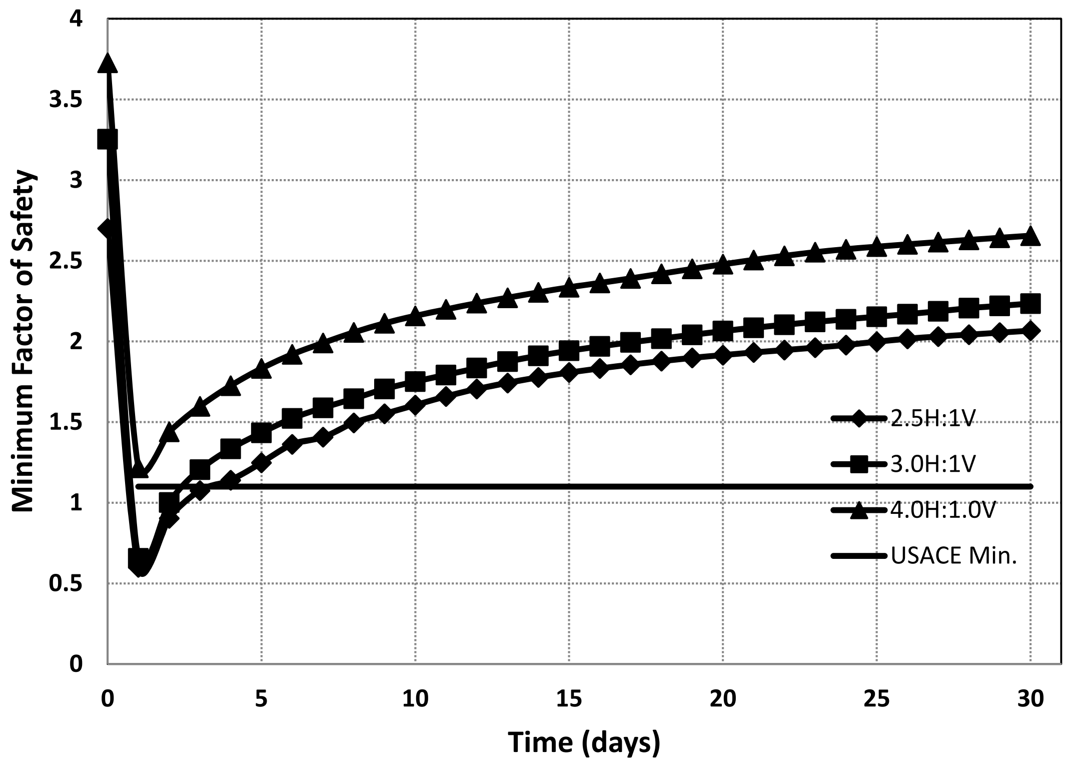

Figure 5-6:Effect of Upstream Slope on Minimum Factor of Safety for Rapid Drawdown

Effect of Unsaturated Shear Strength of Soil on Factor of Safety

The effects of saturated and unsaturated shear strength of soils for upstream slope stability were investigated during rapid drawdown of the reservoir. The drawdown rate of 1m/day which is common condition was selected. Firstly, steady-state analysis was performed and it was seen that saturated zone was larger for unsaturated materials compared to saturated materials. Secondly, transient analysis was performed to obtain the pore water pressure distribution during rapid drawdown. The results shown in Figure 5-6 shows that saturated and unsaturated behavior of materials has similar minimum factor of safety during rapid drawdown. The minimum factor of safety obtained using saturated shear strength materials is slightly higher than calculated from unsaturated shear strength. This decrease in minimum factor of safety from unsaturated materials may be due to having larger wetting zone. Smaller saturated region might dissipate pore water pressure faster than larger saturated zone. As conclusion, the upstream slope of saturated dam materials is more stable than unsaturated dam materials. Clay and embankment materials in earth dams are not fully saturated in the real conditions, unsaturated condition must be take into account for dam design. Moreover, effect of friction angle on min. factor of safety for dam slope stability was investigated. As shown in Fig. Increasing friction angle has increased the stability of earth dam. Friction angle with 10, 20, 30 resulted that earth dam is not stable under these values.

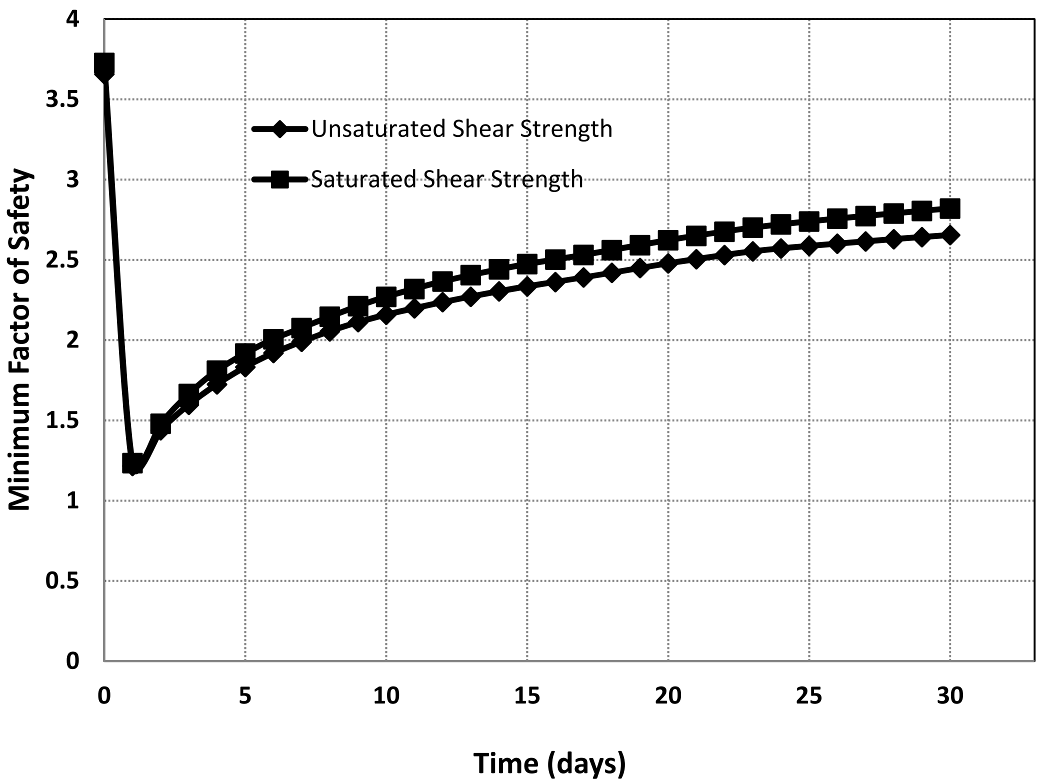

Figure 5-7:Effect of Unsaturated Shear Strength of Soil on Minimum Factor of Safety

Increasing drawdown rate has affected the upstream slope stability. As shown in Figure 5-7 the minimum Factor of safety of the upstream slope of the earth dam increases when the drawdown rate decreases. This is due to the low drawdown rate allows more time for the pore-water pressure dissipation from the saturated zone within the dam. According to Equation 5.1, the dissipation of pore-water pressure increases the shear strength of the dam materials. By means of this, the slope stability increases. On the other hand, the higher drawdown rate will not allow water enough time for pore-water pressure dissipation. So, the shear strength increase in the dam materials is less than that of the materials at a lower drawdown rate. Moreover, the earth dam was not stable for 5m/day drawdown.

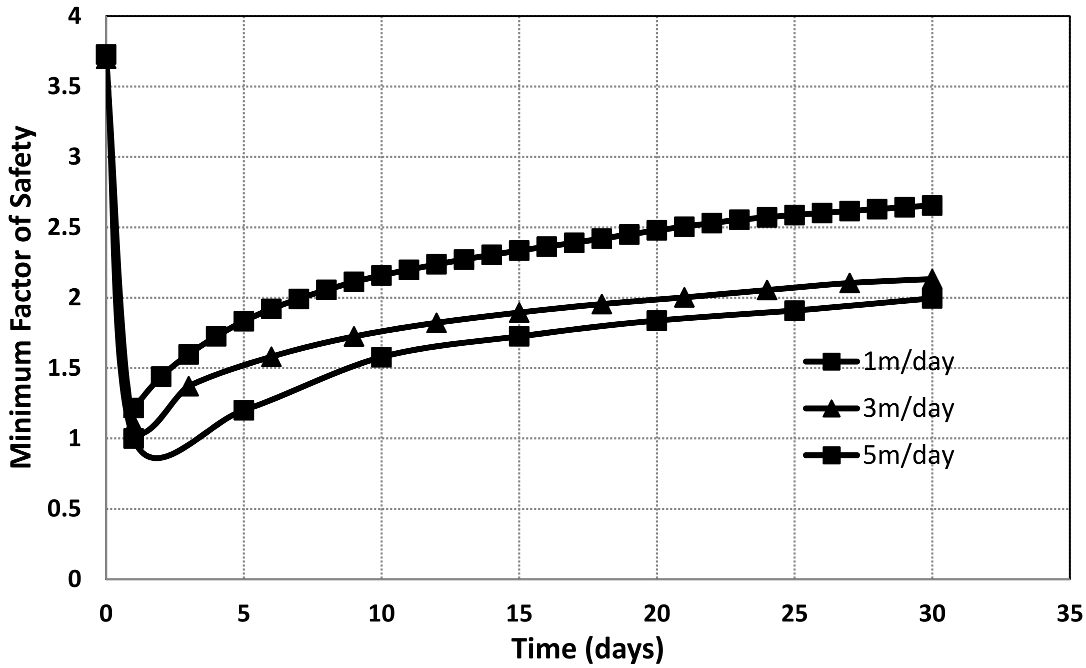

Figure 5-8:Effect of Rapid Drawdown Rate on Min. Factor of Safety

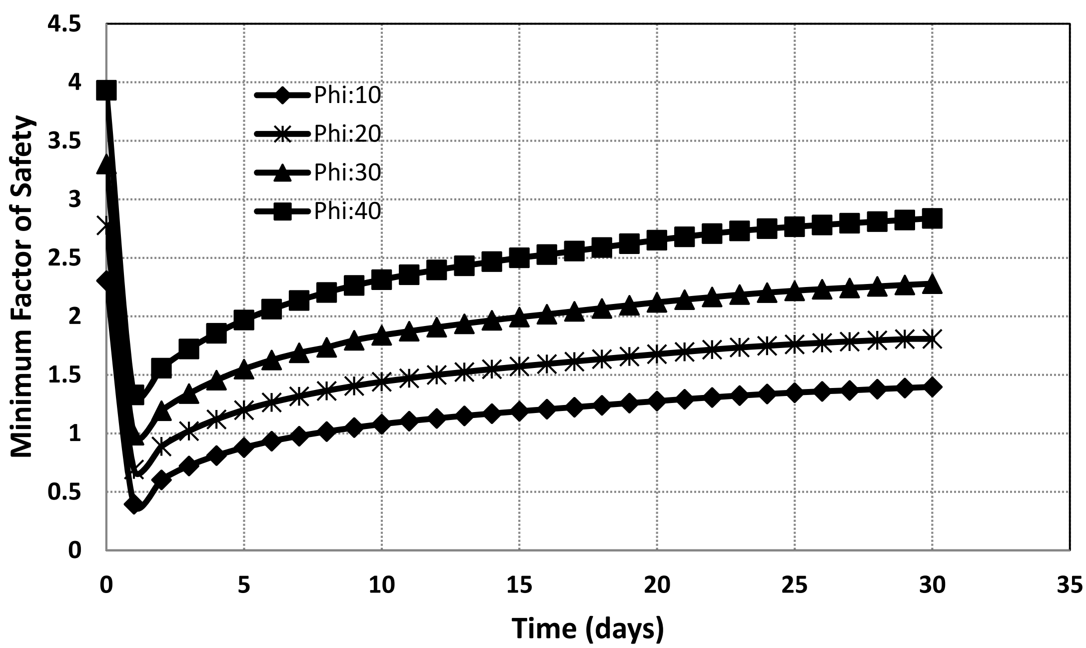

Figure 5-9:Effect of Friction Angle on Min. Factor of Safety

Monitoring Shear Stress in Earth Dam

Monitoring shear stress during rapid drawdown can prevent possible failure of earth dams. Grouted sand which has sensing property under compression was assigned to find a best location in the earth dam. As shown in Figure 5-9 four locations were selected and named Loc.1, Loc.2 for embankment, and Loc.3, Loc.4 for foundation. The dam was analyzed under rapid drawdown condition with 1m/day. Pore-water distribution was obtained from transient analysis. To find a shear stress on grouted sand, shear stress change was obtained from load-deformation analysis. The shear stress change was calculated from full reservoir (0 day) and empty reservoir (30 days later). As shown in Figure 5.11 embankment shear stress change was higher than foundation shear stress change. Loc.1 maximum shear stress change was 92 kPa and it was the highest change among the other locations. With this shear stress change the piezoresistivity was observed around 15.6%. As shown in Figure 5-12 the resistivity change for Loc.2, Loc.3, and Loc.4 were 13.9%, 12%, and 14.4%, respectively. These measurements show that the model is sensitive to shear stress.

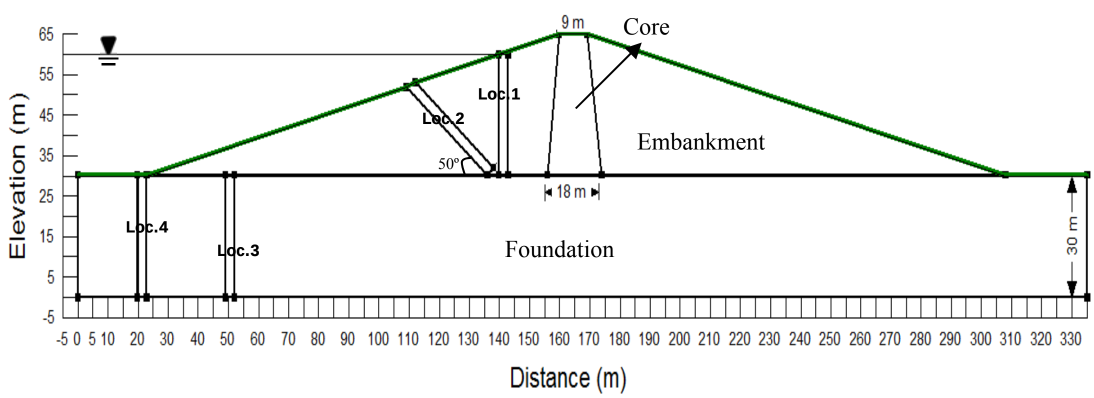

Figure 5-10:Locations for Monitoring Shear Stress in Earth Dam After Rapid Drawdown Condition.

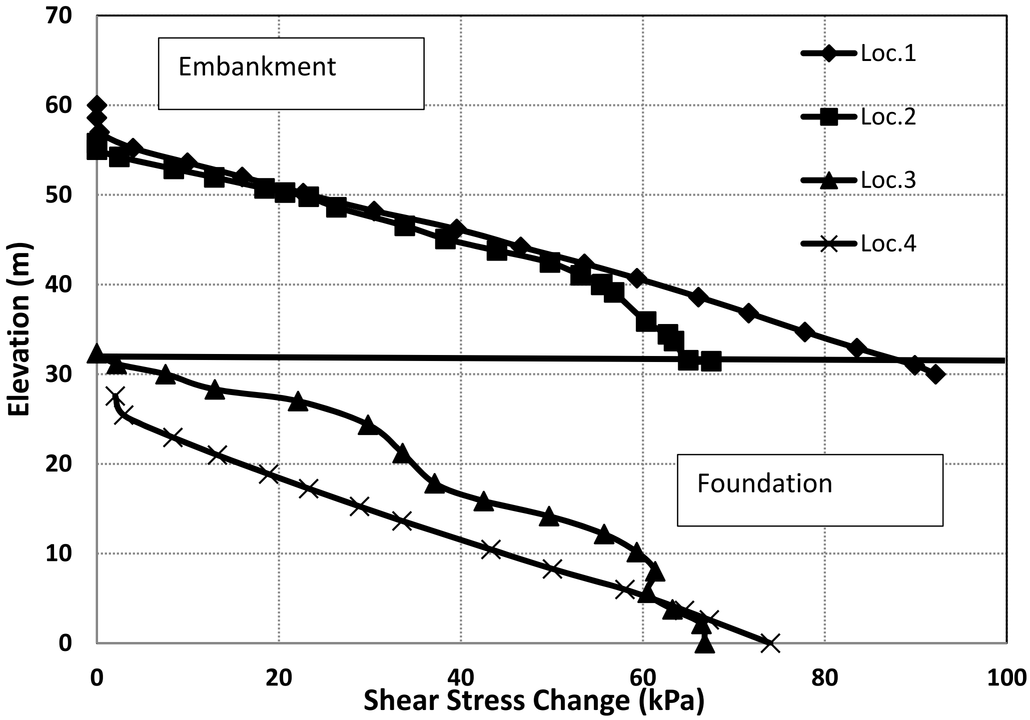

Figure 5-11:Shear Stress Change After Rapid Drawdown

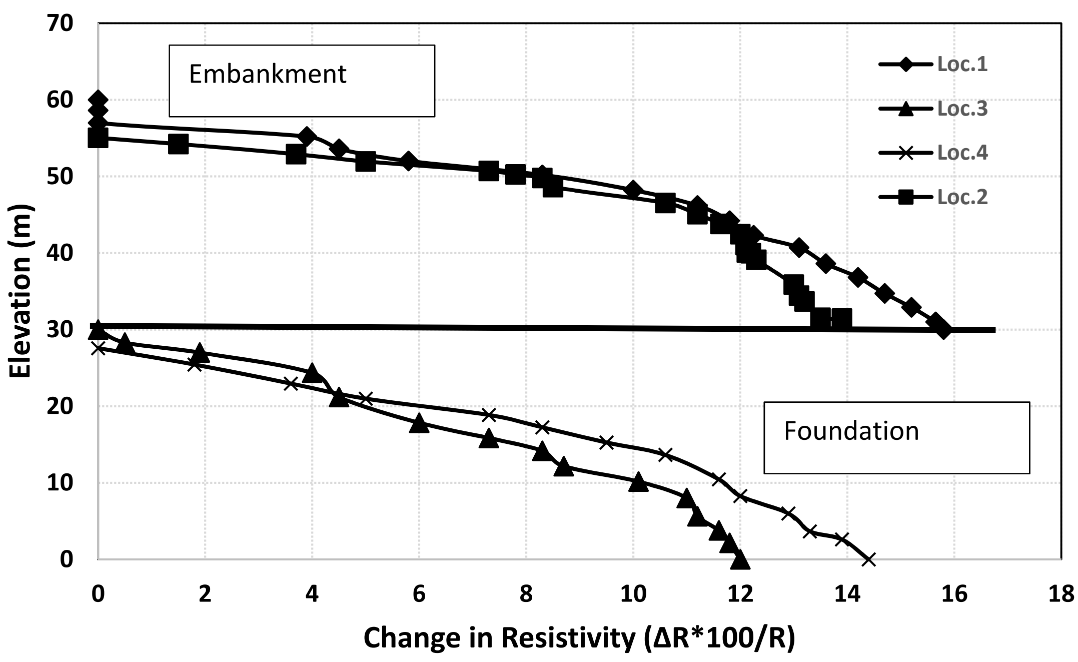

Figure 5-12:Monitoring Shear Stress in Earth Dam During Rapid Drawdown

Seepage Control in the Earth Dam

Since grouted sand has very low permeability value, it was applied in the four locations in the dam for seepage control in Figure 5-13. The locations are upstream face, upstream, core and full body and the values of leakage flow rate were compared to the value obtained from clay core earth dam. As shown in Figure 5.14, location of grouted sand has affected the seepage quantity in the earth dam body and foundation. When it is used for whole body of the earth dam, seepage in the body is almost 0, however using for entire body is not economical. Therefore, seepage decreased from 0.0026 m^3/day/m to 0.00028 m^3/day/m when it is used for upstream. Grouted sand thickness for upstream can be calculated from $t = 0.3 + 0.0035 \times H = 0.45$ m. In this study, 1 m thickness was selected to stay in safe due to unknown effect of water wave. With the application of grouted sand for upstream face, seepage decreased from 0.0025 m^3/day/m to 0.0005 m^3/day/m. When thinking of economical cross-section, upstream face is the best place for earth dam design. Using acrylamide grouted sand for upstream face (1m) in earth dam dropped significantly phreatic line as shown in Figure 5.15. Dropping this line means having lower wetting zone and lower pore-water pressure. This lower pore-water pressure will make the earth dam more stable because it affects the effective stress of the materials in upstream slope. After assigning grouted sand to upstream face, stability analysis was performed. Table 5.8 shows that stability of earth dam also increased after using it for the earth dam. The stability of earth dam increased almost twice under rapid drawdown condition.

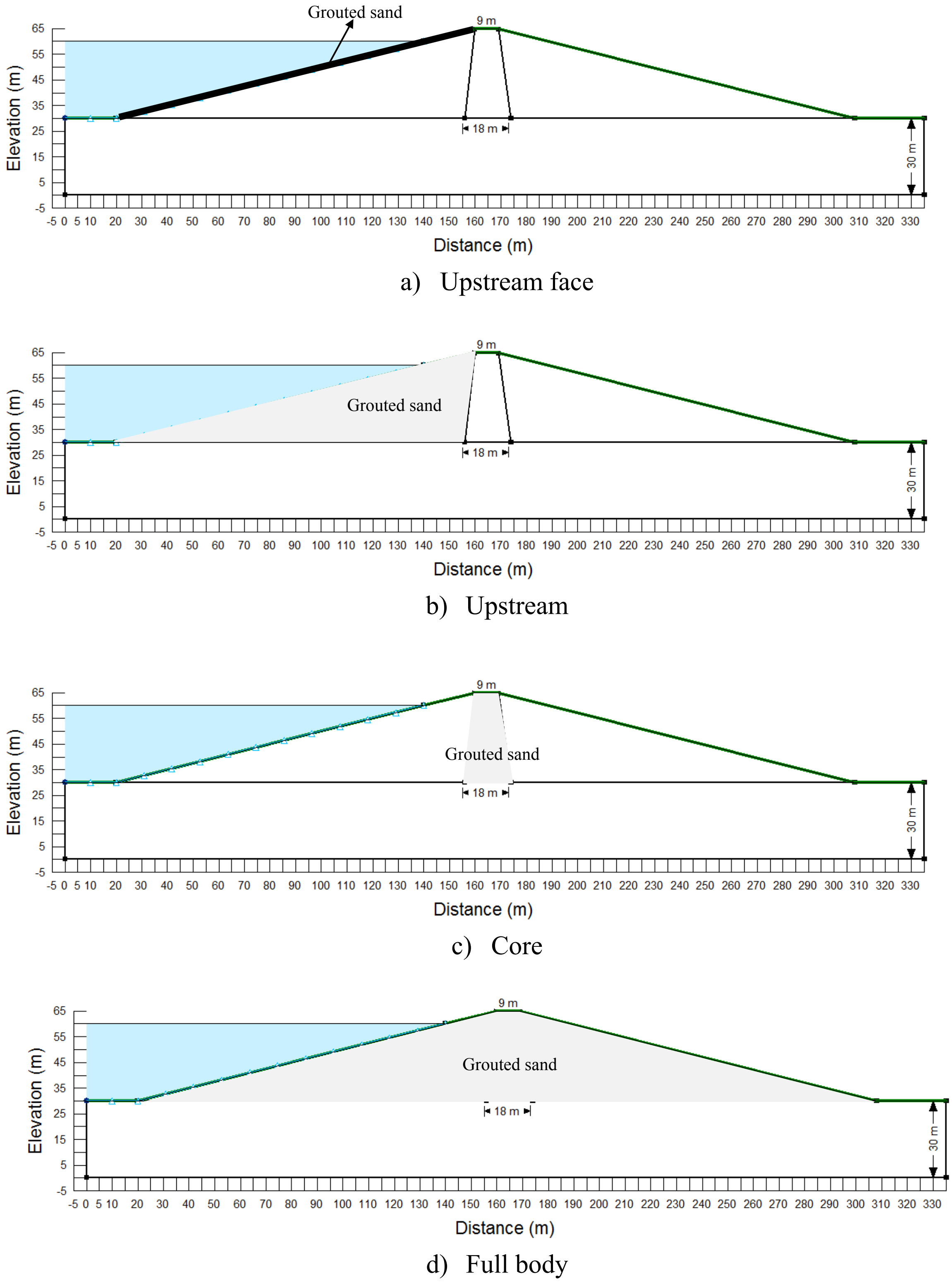

Figure 5-13:Selected Locations in the Earth Dam for Acrylamide Grouted Sand (a) Upstream face, (b)Upstream, (c)Core, and (d)Full body

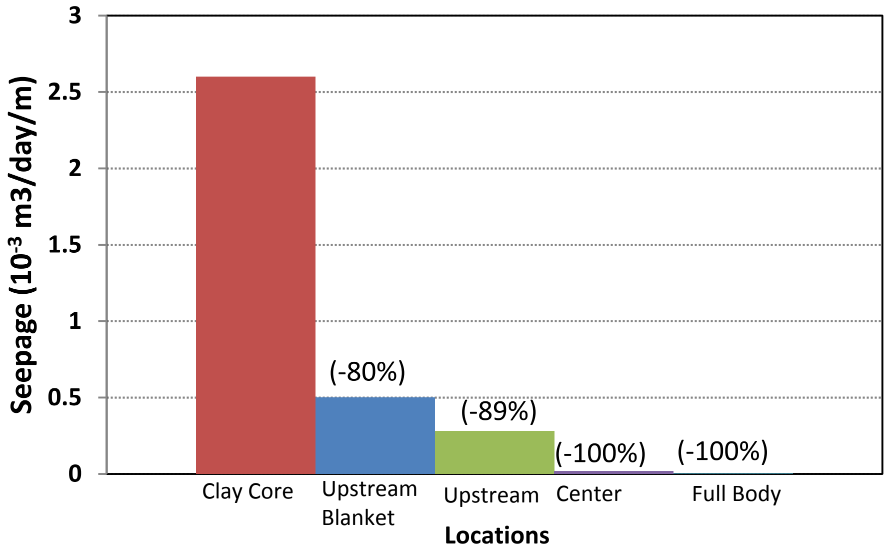

Figure 5-14:Seepage Quantity Changes for Different Locations of Grouted Sands

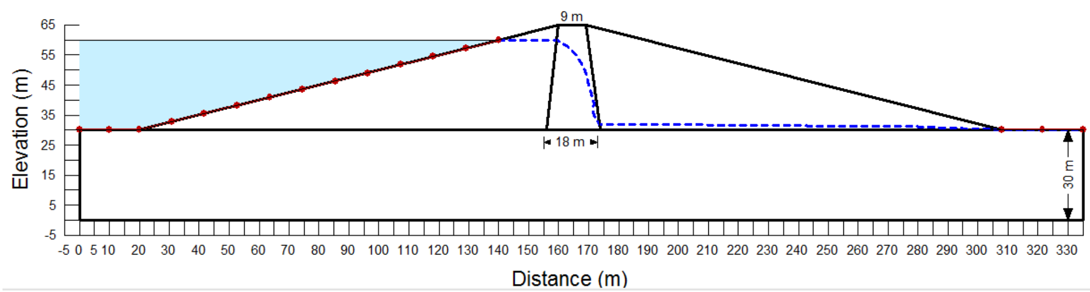

a) Earth dam with clay core

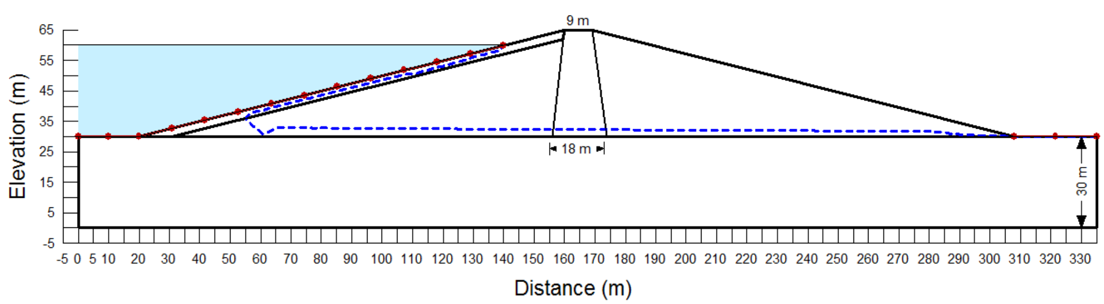

b) Earth dam with acrylamide grouted sand

Figure 5-15:Effect of Acrylamide Grouted Sand on Phreatic Line in the Earth Dam (a) (b)

Table 5-8:Stability of Earth Dam after Using Grouted Sand For Upstream face (1m)

Analysis method	Slope	Zoned type	End of construction		Steady-state		Rapid drawdown
			Upstream	Downstream	Upstream	Downstream	Upstream
Bishop	4.0 H : 1.0 V	Clay core	3.579	3.55	3.677	3.3	1.216
Bishop	4.0 H : 1.0 V	Grouted sand face	3.614	3.55	7.948	3.3	2.359

Summary

Based on the literature review and analysis, following observations are advanced:

1. 2-D plane strain dam was modelled and analyzed under three main conditional. The most severe condition was rapid drawdown condition. Especially, first days of rapid drawdown is more critical. In this condition, max shear stress change in upstream was 94 kPa.

2. Monitoring maximum shear stress in upstream is possible using piezoresistivity method. Since acrylamide grouted sand is sensitivity to compression, acrylamide grouted sand can be used to monitor upstream stability during rapid drawdown.

3. A low rate of reservoir drawdown increases the stability of the upstream slope of the earth dam.

4. Seepage was affected by mesh size of the model. Seepage decreased 29% when mesh size varied from 5mx5m to 1mx1m. Phreatic line was not influenced by mesh size.

5. Unsaturated soil shear strength affected the factor of safety. The slope stability calculated from saturated shear strength is slightly higher than calculated from unsaturated shear strength. Since there will be unsaturated soil in the earth dam during drawdown condition, unsaturated shear strength must be considered for design.

6. Seepage decreased from 0.0026 m3/day/m to 0.0005 m^3/day/m when acrylamide grouted sand was used for upstream face, 80% reduction was observed. Upstream face is the best economical cross-section for usage of acrylamide grouted sand for earth dams. Moreover, using grouted barrier in the earth dam increased the stability twice compared to clay core earth dam.

CHAPTER 6 CONCLUSIONS AND RECOMMENDATIONS

Seepage control in the earth dams is an important task to prevent possible failures. Decreasing phreatic line by using low permeability materials or horizontal drains can be useful to control seepage. When it comes to stability of earth dam, rapid drawdown condition is the most severe condition. So, monitoring shear stress during rapid drawdown condition can provide informations about phreatic line level or possible failures in the upstream. This study was focused on investigation of the behavior of acrylamide grouted sand for earth dams. Since acrylamide grouts has the lowest viscosity (1.2 cP) among all chemical grouts they have been widely used in stopping water in geotechnical engineering. Around 140 acrylamide grouted sands were prepared to investigate the mechanical, permeability and pizeoresistivity properties. Electrical resistivity change was identified as the sensing and monitoring property for the acrylamide grouted sands. 0.1% conductive filler (CF) was added to make the grouted sands very sensing under submerged and moist cured. Nonlinear Vipulanandan p-q piezoresistivity model was used to predict the piezoresistive behavior of the grouted sands.

In this study, earth dam was modelled and grouted using smart acrylamide grouted sand with enhanced piezoresistive properties. Shear stress changes during rapid drawdown was observed.

Conclusions

Based on this study the following conclusions are advanced:

1. Unconfined compressive strength was affected by the density, particle size and gradation. Strength of grouted sands increased when particles are finer. The compressive strength of the grouted sands varied from 240 kPa to 775 kPa after 7days moist curing. Moreover, curing time after 3 days did not affect the mechanical properties of grouted. Vipulanandan p-q model can be used to predict the stress-strain and piezoresistivity behavior of acrylamide grouted sands.

Failure strain and modulus were not influenced by the curing time after 3 days. When grouted sand samples were compacted, the failure strain decreased.

2. The permeability of grouted sand was 10^{-12} m/sec, and it was not affected by grain size distribution and particle size.
3. The acrylamide grouted sand with and without conductive filler were pizoresistive. Adding 0.1% conductive filler into the sand increased the sensitivity of the grouted sands.The average change in resistance change at peak compressive stress was 21% for submerged specimens and 24% for moist cured specimens.
4. 2-D dam was modelled and analyzed under three main conditional. The most severe condition was rapid drawdown condition. Especially, first days of rapid drawdown is more critical. In this condition, max shear stress change in upstream was 94 kPa.
5. Monitoring maximum shear stress change in upstream is possible using piezoresistivity method. Since acrylamide grouted sand is sensitivity to compression, acrylamide grouted sand can be used to monitor upstream stability during rapid drawdown.
6. Seepage was affected by mesh size of the model. Seepage decreased 29% when mesh size varied from 5mx5m to 1mx1m. Phreatic line was not influenced by mesh size.
7. Unsaturated soil shear strength affected the factor of safety. The slope stability calculated from saturated shear strength was slightly higher than calculated from unsaturated shear strength. Since there will be unsaturated soil in the earth dam during drawdown condition, unsaturated shear strength must be considered for design.
8. Seepage decreased from 0.0026 m^3/day/m to 0.0005 m^3/day/m when acrylamide grouted sand was used for upstream face, 80% reduction was observed. Upstream face is the best economical cross-section for usage of acrylamide grouted sand for earth dams.
9. Using acrylamide grouted sand for upstream face incredibly decreased the phreatic line and provide lower wetting region in the earth dam. By means of this, the stability of upstream increased twice compared to clay core earth dam.

Recommendations

1. In this study, a new method for monitoring earth dam during rapid drawdown is presented. The electrical resistivity change was found to be the sensitive property.

2. From the present study, 2-D dam was analyzed under three main conditional. These are end of construction, steady-state and rapid drawdown condition. However, USACE also offers earthquake analysis. The earth dam should be analyzed under earthquake to see the behavior of grouted sand. Moreover, 3-D analysis should be performed to see differences from 2-D analysis.

REFERENCES

AM-9 Chemical Grout Manual. (1965). Cyanamid Company, Number 33166000256370, Washington State Department of Transportation Materials Laboratory Library Olympia, WA 98504-7365.

Billstein, M. Sevensson, U., and Johansson, N. (1999). "Development and Validation of a Numerical Model of Flow through Embankment Dams – Comparisons with Experimental Data and Analytical Solutions." Transport in Porous Media, Vol. 35, No. 3, PP. 395-406.

Bishop, A. W. (1955). "The use of slip circles in stability analysis of slopes." Geotechnique, Vol. 5, No. 1, pp. 7-17

Center for Innovative Grouting Materials and Technology (CIGMAT). (2002a). "Standard Test Method for Measuring Compressive Strength of Grouts and Grouted sands." GR02-02, Univ. of Houston, Houston.

Center for Innovative Grouting Materials and Technology (CIGMAT). (2002b). "Standard Test Method for Permeability of Grouts and Grouted Sands." GR07-02, Univ. of Houston, Houston.

Deniz Ersayin (2006). "Studying Seepage in a Body of Earth-fill Dam by Artificial Neural Nerworks." Master Thesis, Izmir Institute of Technology.

Das, B. M., (1987). "Advanced Soil Mechanics." McGraw-Hill Book Company, New York, U. S. A.

Drochytka, R., Kocianova, M., Cerny, V. (2015). "Development of Grout for Additional Seal Embankment Dams." Procedia Engineering 108 (2015) 632–638

Foster, M., Fell, R., and Spannagle, M. (2000). "A Method for Assessing the Relative Likelihood of Failure of Embankment Dams by Piping." Canadian Geotech. J., 37(5), 1025–1061.

Fellunius, W. (1936). "Calculations of the Stability of Earth Dams." Proceedings of the Second Congress of Large Dams. Vol. 4, pp. 445-63, Washington D. C.

Fredlund DG and Xing A, (1994). “Equations for the soil-water characteristic curve.” Journal of Canadian Geotechnical Journal, vol. 31, pp. 521-532

Garg, S. K. (2006). “Irrigation Engineering and HydraulicStructures,” 19th Edition, Khanna Publishers, Delhi, 42006, pp. 960-1020.

Geo-studio (2012). Stability and Seepage Modeling.Users Guide July Edition, Geo Slope International Ltd., Canada.

General Directorate of State Hydraulic Works, DSI (2012). “Technical Manual for Instrumentations in Dams.” Turkey.

General Directorate of State Hydraulic Works, DSI (2012). “Earth Dam Design Guide.” Turkey.

Harr, M. E. (1962). “Groundwater and Seepage.” McGraw-Hill Book Company, New York, U. S. A.

Gonzalez H.A. and C. Vipulanandan (2005). "Pulse Velocity and Strength Properties of Acrylamide Grouted Sand." CIGMAT Conference Proceeding.

Karol, R. H. (1990). "Chemical Grouting." Marcel Dekker, Inc., New York

Kashef, A. I. (1987). “Groundwater Engineering.” McGraw-Hill Book Company, New York, U. S. A.

Kasim F, Fei W. S. (2002). “Numerical Parametric Simulations for Seepage Flow Behaviour Through an Earthfill Dam.” Journal of Civil Engineering 14(1), Malaysia.

Knight, M. A. (2016). “Construction Monitoring For Earth Dams [PowerPoint slides].” Retrieved from http:// www.civil.uwaterloo.ca/

Lane, P. A., and Griffiths, D. V. (2000). “Assessment of Stability of Slopes Under Drawdown Conditions.” Journal of Geotechnical and Geonvironmental Engineering, 126(5):443-450.

Linsley R.K. and Franzini, J.B., (1964). “Water-Resources Engineering.” McGraw – Hill, Tokyo, pp. 173-211.

Morgenstern, N. R. and Price, V. E. (1965). “The Analysis of the Stability of General Slip Surfaces.” Geotechnique, Vol. 15, No. 1 pp. 77-93.

Narduzzo, L. (Feb. 2003). “The Toronto Transit Commision’s Subway Tunnel and Station Leak Remediation Grouting Program,” Grouting and Ground Treatment, GSP No. 120, Vol.2, pp.1617-1627.

Narita, Kunitomo, (2005). “Design and Construction of Embankment Dams.” Department of Civil Eng., Aichi Institute of Technology.

Noori B. M. A., Ismaeel K. S. (2011). “Evaluation of seepage and stability of Duhok Dam.” Al-Rafidain Engineering 19(1): 42-58, Iraq.

Novak, P., Moffat, A.I.B., Nalluri, C. and Narayanan R. (2001). “Hydraulic Structures Fourth Edition.” Tylor & Francis Group, London.

Osuji, S. O. and Adegbemileke, S. A. (2015). “Phreatic Line and Pore Pressure Stresses in Zoned Rockfill Dam.” Asian Journal of Science and Technology, Vol.6, Issue 0.5, pp. 1447-1454

Ozgurel, H. G. and Vipulanandan, C. (2005). "Effect of Grain Size Distribution on Permeability and Mechanical Behavior of Acrylamide Grouted Sand." Journal of Geotechnical and Geoenvironmental Engineering, Vol. 131, No. 12, pp.1457-1465

Pinyol, NM, Alonso EE and Olivella S. (2008). “Rapid drawdown in slopes and embankments.” Water Resources Research, vol. 44, pp. 1-22.

Sakamoto, T., Yoshida, H., Yamaguedi, Y, (2002). “Numerical Simulation of Sliding of an Earth Dam During 1995 Kobe Earthquake.” The 22nd USSD Annual Conference, JAPAN, 2002.

Sarma, S. K. (1973). “Stability Analysis of Embankment and Slopes.” Geotechnique, Vol. 23 (3), pp.423-33.

Seepage Modeling with SEEP/W (2012). “SEEP/W Manual 2012”.

Souliyavong T., (2012). “Factors Affecting the Stability Analysis of Earth Dam Slopes Subjected to Reservoir Drawdown.” Second International Conference on Geotechnique, Construction Materials and Environment, Kuala Lumpur, Malaysia, Nov. 14-16, 2012.

Spencer, E. (1967). “A method of Analysis of the Stability of Embankments, Assuming Parallel

Interslice Forces." Geotechnique, Vol. 17, pp. 11-26.

Suhail, A, Khattab A. (2008). "Stability Analysis of Mosul Dam under Saturated and Unsaturated Soil Conditions." Al-Rafidain Engineering Vol. 18, No.1.

Tallard, G. R., Caron, C. (1977). "Chemical Grouts for Soils Vol.1 Available Materials," Federal Highway Administration Report, Report # FHWA-RD-77-50.

USACE (1993). "Engineer and Design; Seepage Analysis and Control for Dams." EM 1110-2-1901, U. S. Army Corps of Engineers, Washington, U. S. A.

USACE (1994). "Deformation Monitoring and Control Surveying." EM-110-2-1004, US Army Corps of Engineering, Washington, DC.

USACE (1995). "Instrumentation of Embankment Dams and Levees." EM-110-2-1908, U. S. Army Corps of Engineering, Washington, DC

USACE (1997). "Chemical Grouting." Technical Engineering and Design Guides No.24.

USACE (2004). "General Design and Construction Considerations for Earth and Rockfill Dams." Department of the Army, U.S. Army Corps of Engineers, Washington DC, United States of America.

USBR (1960). "Design of Small Dams." United States Department of the Interior of Bureau Reclamation, Denver, Colorado, First Edition.

USBR (1987). "Design of Small Dams." United States Department of the Interior of Bureau Reclamation, Denver, Colorado, Third Edition.

USBR (1992). "Embankment Design." United States Department of the Interior of Bureau Reclamation, Denver, Colorado.

www.asctec.de/en/drone-uav/uav-uas-drone-bridge-dam-inspection.

Vanapalli SK, Fredlund DG, Pufahl DE and Clifton AW, (1996). "Model for the Prediction of Shear Strength with Respect to Soil Suction." Canadian Geotechnical Journal, vol.3, pp. 379-392

Vipulanandan, C., and Paul, E. (1990). “Performance of epoxy and polyester polymer concrete.” ACI Mater. J., 873(3), 241–251.%d